ARTICLE | OPEN ACCESS

Drug Discovery

To Cite:
Abdelgaid HA, Ibrahim KA. Molecular docking study for the interaction behavior of human acetylcholinesterase catalytic activity with common organophosphate pesticides. *Drug Discovery* 2026; 20: e7dd3053
doi:

Author Affiliation:
[1]Egyptian Center for Disease Control (CDC), National Hepatology and Tropical Medicine Research Institute (NHTMRI), Corniche El Nil - Imbaba – Giza, P.O. BOX 12651, Egypt.
[2]Mammalian Toxicology Department, Central Agricultural Pesticides Laboratory, Agricultural Research Center, Dokki, Giza, 12618, Egypt.

***Corresponding Author:**
Khairy A. Ibrahim,
Mammalian Toxicology Department, Central Agricultural Pesticides Laboratory, Agricultural Research Center, Dokki, Giza, 12618, Egypt.
Email: khairy_moneim@yahoo.com; drkhairyibrahim@gmail.com
ORCID: https://orcid.org/0000-0002-6437-8809

Peer-Review History
Received: 07 July 2025
Reviewed & Revised: 03/August/2025 to 09/February/2026
Accepted: 16 February 2026
Published: 27 February 2026

Peer-Review Model
External peer-review was done through double-blind method.

Drug Discovery
pISSN 2278–540X; eISSN 2278–5396

Molecular docking study for the interaction behavior of human acetylcholinesterase catalytic activity with common organophosphate pesticides

Hala A Abdelgaid[1], Khairy A Ibrahim[2]*

ABSTRACT

Organophosphate pesticides (OPs) are the most commonly used pesticides and act as key inhibitors of acetylcholinesterase (AChE). However, their mechanism of action in human AChE (hAChE) is not well studied. The recent release of new 3D structures of hAChE in the NCBI database prompted us to investigate their interactions with the enzyme's catalytic active site. We used an in silico molecular docking approach with AutoDock Vina to study the interactions of thirty common OPs with a new hAChE structure (6WUZ). The binding energies of the lowest-energy poses were determined to select conformers for further analysis. Based on interactions with Ser203 and His447, our study divided the OPs into three groups of hAChE inhibitors. The first group comprised eight OPs that interacted with both Ser203 and His447 at the catalytic active site, suggesting strong inhibition with docking energy ranging from −7.6 to −5.1 kcal/mol. The second group comprised nine compounds that did not interact with Ser203 but interacted with His447, suggesting medium inhibition with docking energy ranging from −7.9 to −5.2 kcal/mol. The third group comprised thirteen compounds that did not interact with either His447 or Ser203, with docking energy ranging from −7.5 to −4.5 kcal/mol, and were expected to be weak hAChE inhibitors. In conclusion, the studied OPs exhibit distinct interaction behaviors with hAChE, which may help us understand their toxicity and inform the development of new strategies for AChE reactivators after OP exposure and for the treatment of neurodegenerative disorders.

Keywords: Organophosphates, Human Acetylcholinesterase, Active Site, Autodock Vina, Free Energy.

1. INTRODUCTION

Organophosphates (OPs) are commonly used in agriculture, farm cultivation, veterinary medicine, and public hygiene to control pathogens (routes) of diseases (Mdeni et al., 2022). Their leftovers are leaching into the soil, groundwater, and aquatic food webs as a result of overexploitation. Subsequently, OPs can induce

different types of toxicity in insects, plants, animals, and humans (Mangas et al., 2017). The primary neurotoxic mechanism of Ops, which tends to harm the normal structure and function of the brain and neurological system, is the suppression of acetylcholinesterase (AChE, EC 3.1.1.7) activity (Ibrahim et al., 2021).

As an enzyme, AChE's primary physiological role is to terminate chemical transmission at cholinergic synapses by hydrolyzing the neurotransmitter acetylcholine (ACh) into choline and acetate at a high turnover rate (Shakil et al., 2011). Therefore, OPs can irreversibly inhibit AChE by forming a covalent bond with a serine residue at the catalytic active site (Kumar et al., 2018). Moreover, loss of AChE activity causes ACh accumulation, leading to a cholinergic crisis with toxic and potentially lethal outcomes (Lindgren et al., 2022).

The mechanism of action and structure of AChE were derived from the crystal structure of the enzyme (Kiametis et al., 2017). In this issue, X-ray crystallographic structures of AChE (over 100 structures) have been published in the Protein Data Bank (PDB) from different species with covalent or reversible inhibitors. Furthermore, most of those structures are gained from the mouse or the electric ray (Torpedo californica) homologs, and a few human AChE (hAChE) structures have been solved to date (Ekström et al., 2022).

A recent study showed that the catalytically active site of hAChE is a deep, narrow gorge that constitutes the peripheral anionic site (PAS), enhancing the entry of choline esters into the catalytic active site (CAS) (Lindgren et al., 2022). With a catalytic triad and anionic subsites, CAS is located close to the bottom of the gorge. The catalytic triad is involved in the ACh hydrolysis, while the anionic subsite is the choline-binding pocket (Saxena, 2019). The peripheral site offers a mild allosteric stimulation of the acylation process and increases catalytic efficiency (Cheung et al., 2012). There are two adjacent areas of the catalytic triad, known as the acyl pocket and oxyanion hole, that participate in positioning of the substrate for attack by the catalytic triad (Rosenfeld and Sultatos, 2006; Saxena, 2019).

The catalytic triad is mainly composed of Ser203, His 447, and Glu334 (Cheung et al., 2012; Lindgren et al., 2022), which partially differ between different crystal structures of hAChE complexed ligands. The Glu334 position has replaced by Glu202 in the recent X-ray crystallographic structures (Ekström et al., 2022), and the anionic subsite consists mainly of Trp86 (Lindgren et al., 2022). The acyl pocket of the hAChE active gorge mainly comprises Phe295 and Phe297, while the oxyanion hole subsite mainly contains Gly120 (Cheung et al., 2012), Gly121, Gly122, and Ala204 (McGuire et al., 2021; Lindgren et al., 2022).

Consequently, it becomes a necessity to estimate the behavioral interaction of AChE inhibitors, which may provide new strategies for protecting against OP poisoning and may lead to improved therapeutics for treating cholinergic-related diseases (Cheung et al., 2012). Hence, the key aim of the present study is to study the behavioral interaction of thirty common OPs with hAChE to evaluate their selectivity with the enzyme active sites gorge (PAS and/or CAS) and obtain more information about their toxicity properties when absorbed in the human organism.

2. MATERIALS AND METHODS

2.1. Preparation of hAChE as a target receptor

The ligand-bound X-ray crystal structure of hAChE (PDB ID: 6WUZ) was selected with a 2.25 Å resolution, and Rwork/Rfree of 0.168/0.190 (McGuire et al., 2021), and the validation parameters suggested the good quality of the modeled structure. The protein molecule was first prepared by eliminating water, ligands, heteroatoms, and chain B. Then, using AutoDockTools (Version 1.5.7), polar hydrogen and charge were added to the macromolecule.

2.2. Preparation of ligands

The 3D structures of thirty common OPs compounds (Kumar et al., 2018) were downloaded from PubChem and their CID numbers are Isofenphos (CID: 32872), Tetrachlorvinphos (CID: 5284462), Azamethiphos (CID: 71482), Methylparathion (CID: 4130), Malathion (CID: 4004), Monocrotophos (CID: 5371562), Dimethoate (CID: 3082), Acephate (CID: 1982), Triazophos (CID: 32184), Azinphosmethyl (CID: 2268), Quinalphos (CID: 26124), Chlorpyrifos (CID: 2730), Parathion (CID: 991), Fenthion (CID: 3346), Cadusafos (CID: 91752), Ethion (CID: 3286), Dichlorvos (CID: 3039), Phosmet (CID: 12901), Coumaphos (CID: 2871), Fenamiphos (CID: 31070), Fenitrothion (CID: 31200), Diazinon (CID: 3017), Dicrotofos (CID: 5371560), Profenofos (CID: 38779), Naled (CID: 4420), Chlorpyrifos-methyl (CID: 21803), Ethoprophos (CID: 3289), Phosphamidon (CID: 3032604), Phorate (CID: 4790) and Terbufos (CID: 25670). Molecular geometry was optimized, and appropriate charges were then assigned to optimize the structure of ligands using Open Babel (O'Boyle et al., 2011).

2.3. Protein-ligand docking

The target protein and ligand were docked using AutoDock Vina (Trott and Olson 2010). Docking was carried out with a box volume of 64.00 × 68.00 × 62.00 Å with a center of 41.735, 46.131, and 352.204. Throughout the docking study, the flexible ligands searched their complementary site(s) within the search space of rigid macromolecules. Ligands with the lowest binding affinity and promising binding pose were chosen as the best conformation. The interactions of protein residues with ligands were analyzed by Discovery Studio Visualizer v21.1.0.20298 (BIOVIA, Dassault Systèmes, 2020). Initially, Sarin was extracted from the receptor and re-docked into the hAChE t binding pocket to validate the docking method. The root mean square deviation (RMSD) between the docked and experimental Sarin revealed that the first pose of Sarin nearly superimposes (RMSD < 1) with the experimental structure of Sarin (Figure 1). Thus, the docking method was reasonably accurate and reproducible. Furthermore, we analyzed 10 runs of Vina docking and the interaction probability of each OP compound with important amino acids in the hAChE active site (on each run) at the lowest energy pose (1st pose) was recorded, then the lowest conformers were selected for further analysis.

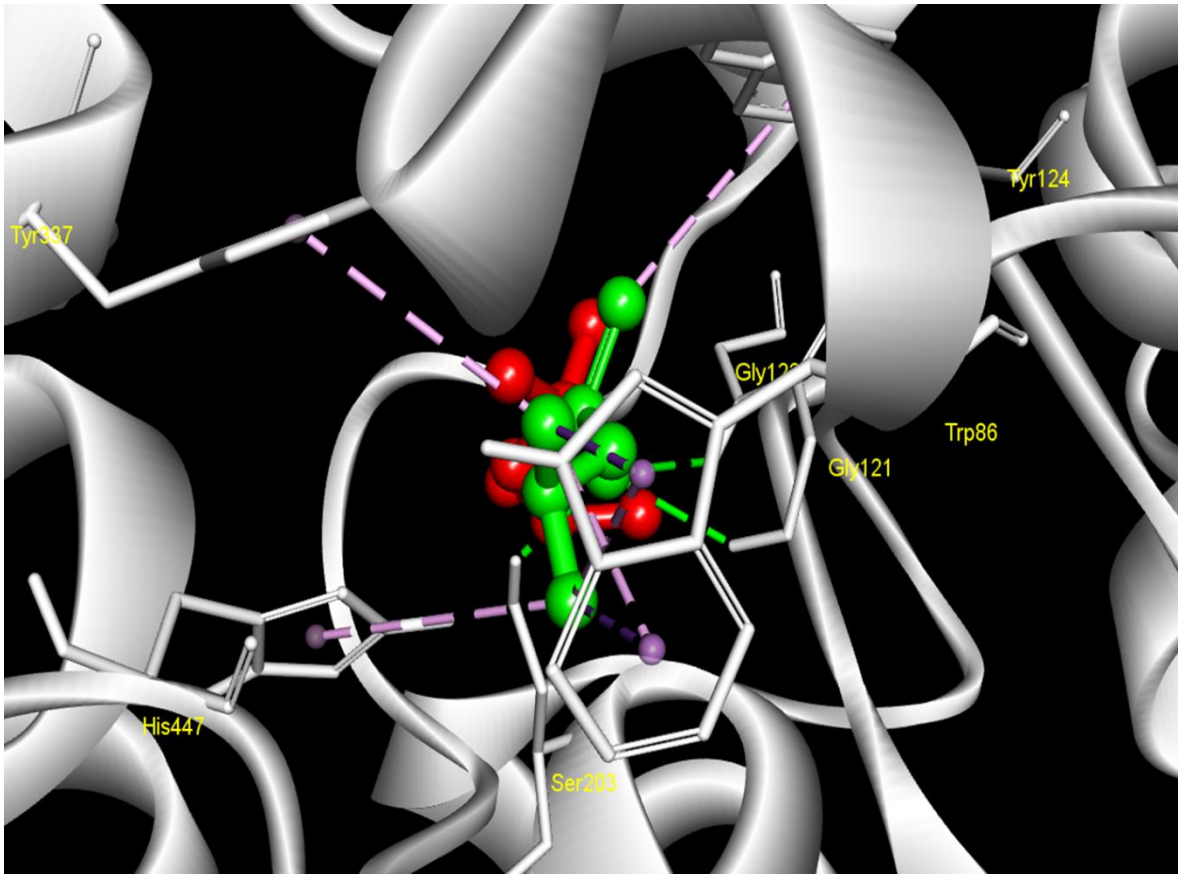

Figure 1: Validation of molecular docking method using Sarin ligand extracted from the 3D structure of hAChE (6WUZ: white): Experimental sarin (red) and docked sarin (green).

3. RESULTS AND DISCUSSION

3.1. Probabilities of OPs interaction with specific amino acids in the hAChE active site

The probabilities of the thirty studied OPs to interact with hAChE (Table 1) are trended to the amino acids from CAS (Ser203 and His447) and PAS (Phe338, Tyr337, Tyr124, Trp286, and Tyr341) at the lowest energy pose i.e., first pose (RMSD = 0). Our results newly classified OPs compounds into three groups according to their interaction with active site amino acids Ser203 and His447. The first one comprised eight OPs compounds (Isofenphos, Tetrachlorvinphos, Azamethiphos, Methylparathion, Malathion, Monocrotophos, Dimethoate, and Acephate), which interacted with both Ser203 and His447. They were arranged according to the docking free energy, where the formed Isofenphos-hAChE complex recorded the lowest energy (–7.6 to –6.6 kcal/mol), and Acephate-hAChE was the highest one (–5.1 to –4.3 kcal/mol). All OPs in this group interacted with CAS and PAS, where Methylparathion and Monocrotophos scored the highest interaction probabilities with CAS (Table 1). Our results suggested that those eight OPs are more toxic and might

irreversibly inhibit hAChE. This goes in line with Lindgren et al., (2022), who showed that the strong OPs compounds impair the function of hAChE by acting as selective electrophiles that react with the catalytic serine to form a covalent bond and various non-covalent interactions with other amino acid residues.

Table 1: Probabilities of the interaction of OPs with specific amino acids on hAChE active site gorge at the first docking pose/10 Vina docking runs.

Name	SER 203	HIS 447	PHE 338	TYR 337	TYR 124	TRP 286	TYR 341
OPs interacted with Ser203 and His447							
Isofenphos	1	1	2	1	1	9	7
Tetrachlorvinphos	1	1	8	0	8	9	9
Azamethiphos	1	1	4	3	3	3	3
Methylparathion	3	5	1	3	5	4	6
Malathion	1	2	6	2	4	6	8
Monocrotophos	3	4	1	0	2	2	3
Dimethoate	1	1	1	0	0	0	0
Acephate	1	2	0	2	3	0	0
OPs interacted with His447							
Triazophos	0	3	1	3	4	10	10
Azinphosmethyl	0	3	2	4	7	10	10
Quinalphos	0	1	0	0	9	10	10
Chlorpyrifos	0	1	8	0	5	10	10
Parathion	0	2	0	2	3	8	10
Fenthion	0	3	6	1	3	9	9
Cadusafos	0	1	1	1	1	5	3
Ethion	0	2	2	2	2	0	2
Dichlorvos	0	6	0	6	5	0	0
OPs interacted not interacted with Ser203 and His447							
Phosmet	0	0	6	3	7	10	10
Coumaphos	0	0	3	1	2	7	6
Fenamiphos	0	0	7	3	8	9	9
Fenitrothion	0	0	0	0	0	9	9
Diazinon	0	0	0	8	7	10	9
Dicrotofos	0	0	0	0	2	1	1
Profenofos	0	0	0	0	0	10	10
Naled	0	0	3	2	2	2	2
Chlorpyrifos-methyl	0	0	3	0	2	8	8
Ethoprophos	0	0	2	2	3	3	2
Phosphamidon	0	0	0	0	0	0	0
Phorate	0	0	1	1	1	2	1
Terbufos	0	0	0	0	0	3	1

The second group comprised nine OPs (Trsiazophos, Azinphosmethyl, Quinalphos, Chlorpyrifos, Parathion, Fenthion, Cadusafos, Ethion, and Dichlorvos). They did not interact with Ser203, but they interacted with His447, where the Triazophos-hAChE complex recorded the lowest energy (–7.9 to –6.9 kcal/mol), and Dichlorvos-hAChE scored the highest energy (–5.0 to –3.9 kcal/mol). All OPs in this group interacted with CAS at His447 and PAS, where Dichlorvos scored the highest number of His447 interaction probabilities

(Table 1). We supposed that those OPs are less toxic than the first group and might have a little degree of hAChE inhibition, but may be converted to strong inhibitors when interacting with the adjacent residue (Ser203).

The third group comprised thirteen OPs (Phosmet, Coumaphos, Fenamiphos, Fenitrothion, Diazinon, Dicrotofos, Profenofos, Naled, Chlorpyrifos-methyl, Ethoprophos, Phosphamidon, Phorate, and Terbufos). They neither interacted with Ser203 nor His447, and all of them interacted with PAS amino acids, except Phosphamidon. They arranged from Phosmet (–7.5 to –5.8 kcal/mol) to Terbufos (–4.5 to –4.3 kcal/mol) (Table 1). We supposed that this group has the lowest toxicity of the thirty studied OPs and might interact with hAChE via a reversible reaction. In this regard, Saxena (2019) reported that the binding of any ligand at PAS blocks the entry of substrates and the exit of the products from the base of the active site. Also, some ligands can bind with PAS and hence block the entrance of Ach in the catalytic gorge to partially inhibit the activity of AChE.

We also noticed that the most researched Ops' interaction probabilities with Tyr241 and Trp286 can be higher than those with Tyr124, Phe338, and Tyr337. Even said, PAS amino acids vary depending on the ligand and are not fixed (Cheung et al., 2012), Tyr337, Phe338, and Tyr124 on PAS in hAChE, coupled with nerve agents (McGuire et al., 2021; Lindgren et al., 2022), as well as Trp286 and Ty341 are trending and forming stacking interactions with most ligands (Ekström et al., 2022).

Table 2: Molecular docking results showing OPs compounds that interacted with hAChE active site His447 as well as Ser203 at the lowest energy poses.

Name	Energy (kcal/mol)	Interactive amino acids
Isofenphos	-7.6	HIS447, SER203, TRP86, TYR337, TYR72, TYR124 and TYR341
Tetrachlorvinphos	-7.1	HIS447, SER203, TRP86 and TYR124
Azamethiphos	-6.9	HIS447, SER203, GLU202, TRP86, PHE338, TYR337, TYR124 and TYR341
Methylparathion	-6.4	HIS447, SER203, GLU202, TRP86, PHE338 and TYR124
Malathion	-6.4	HIS447, SER203, GLU202, PHE297, PHE338, TYR124, ASP74 and SER125.
Monocrotophos	-6.1	HIS447, SER203, GLU202, TRP86, GLY121 and SER125.
Dimethoate	-5.2	HIS447, SER203, GLU202, TRP86, PHE338, and SER125
Acephate	-5.1	HIS447, SER203, GLU202, TRP86, GLY121, TYR133 and GLY448

3.2. Analysis of lowest energy conformers of OPs in the first group (interacted with Ser203 & His447)

3.2.1. Docking of Isofenphos into hAChE

The selected Isofenphos-hAChE complex (-7.6 Kcal/mol) stabilized by many types of interactions. Isofenphos interacted with the CAS catalytic triad at Ser203 and His447 via conventional hydrogen bond and Pi-Sulfur interaction, respectively, as well as hydrophobic interaction (Pi-Sigma) with Trp86 CAS anionic subsite. Also, Isofenphos formed the hydrophobic interactions with the more common PAS amino acids involving Tyr337 (Pi-Pi T-shaped), Tyr124 (Pi-alkyl), and Tyr341 (Pi-alkyl). Although the Tyr72 residue of PAS is involved in interaction via a Pi-alkyl hydrophobic bond (Figure 2, left), other residues became (Table 2) closer to the pesticide without interactions (Phe338, Gly121, Tyr133, Asp74, Asn87, Gly448, and Ser125) (Figure 2, right).

3.2.2. Docking of Tetrachlorvinphos into hAChE

The selected Tetrachlorvinphos-hAChE conformer (-7.1 Kcal/mol) stabilized via many types of interactions. Tetrachlorvinphos interacted with Ser203 via a hydrogen bond and with His447 via a conventional hydrogen bond and a carbon-hydrogen bond (H-donor) as well as Trp86 via a hydrophobic bond (Pi-Pi Stacked). Although Tetrachlorvinphos interacted with PAS at Tyr124 only via a carbon-hydrogen bond (Table 2) & (Figure 3, left), other residues became closer without interactions (Phe338, Phe297, Gly120, Gly121, Gly122, Tyr133, Tyr337, Asp74, Asn87, Gly448, and Ser125) (Figure 3, right).

3.2.3. Docking of Azamethiphos into hAChE

The selected Azamethiphos-hAChE conformer (-6.9 Kcal/mol) stabilized via many interaction types at the CAS catalytic triad (Ser203/His447/Glu202) and anionic subsite (Trp86). In this respect, Azamethiphos bound with Ser203 via a conventional hydrogen

bond, His447 via three interactions (conventional hydrogen, carbon-hydrogen, and Pi-sulfur), Glu202 via an electrostatic bond (attractive charge), and Trp86 via a hydrophobic (Pi-Sigma) interaction. Moreover, Azamethiphos forms many hydrophobic interactions with PAS amino acids residue; Phe338 (Pi-Alkyl), Tyr337 (Pi-Pi T-shaped), Tyr124 (Pi-Pi T-shaped), and Tyr341 (Pi-Pi T-shaped and Pi-Alkyl) (Table 2) & (Figure 4, left). Other amino acid residues became closer to the pesticide without interactions involving Phe295, Phe297, Gly120, Gly121, Tyr133, Asp74, and Gly448 (Figure 4, right). These results suggested that Phe295 and Phe297 may form the acyl pocket (Saxena, 2019) as well as Gly120 and Gly121 form an oxyanion hole (McGuire et al., 2021).

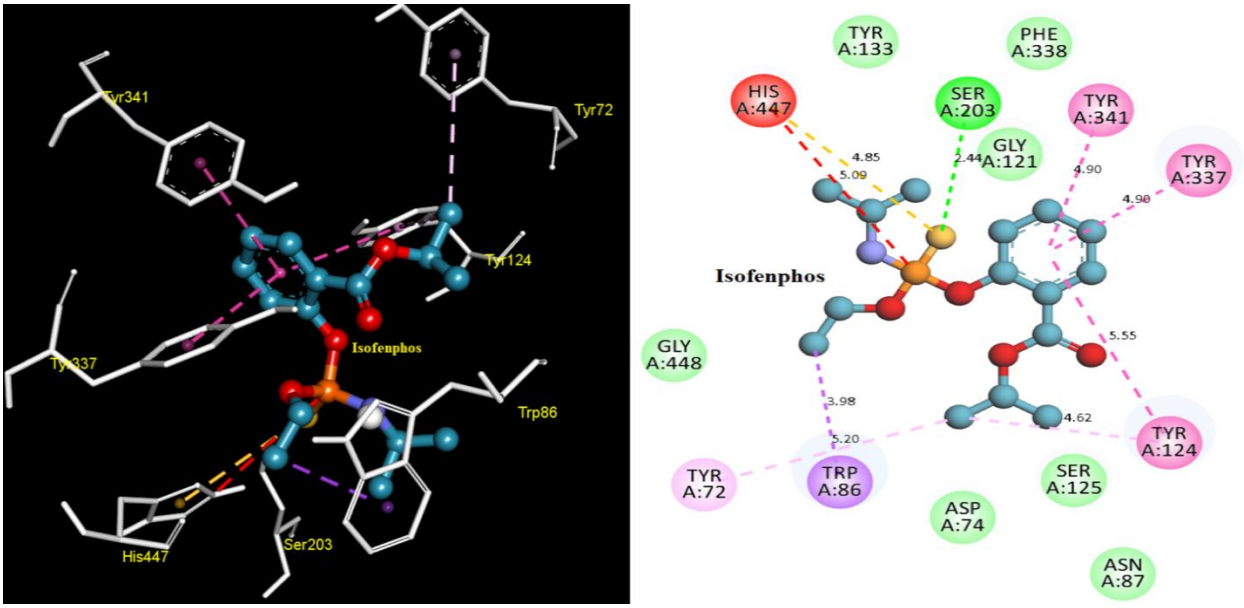

Figure 2: Interaction of Isofenphos with hAChE active site: 3D structure of Isofenphos-hAChE (left) and 2D structure (right) indicating types of interactions.

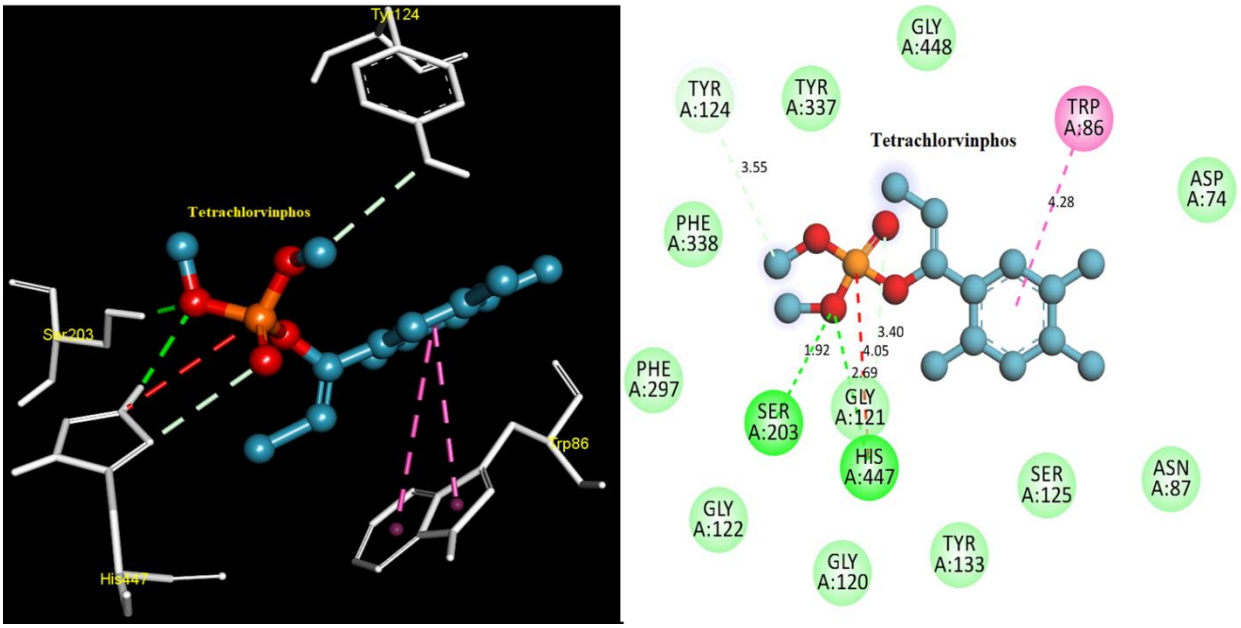

Figure 3: Interaction of Tetrachlorvinphos with hAChE active site: 3D structure of Tetrachlorvinphos-hAChE (left) and 2D structure (right) indicating types of interactions.

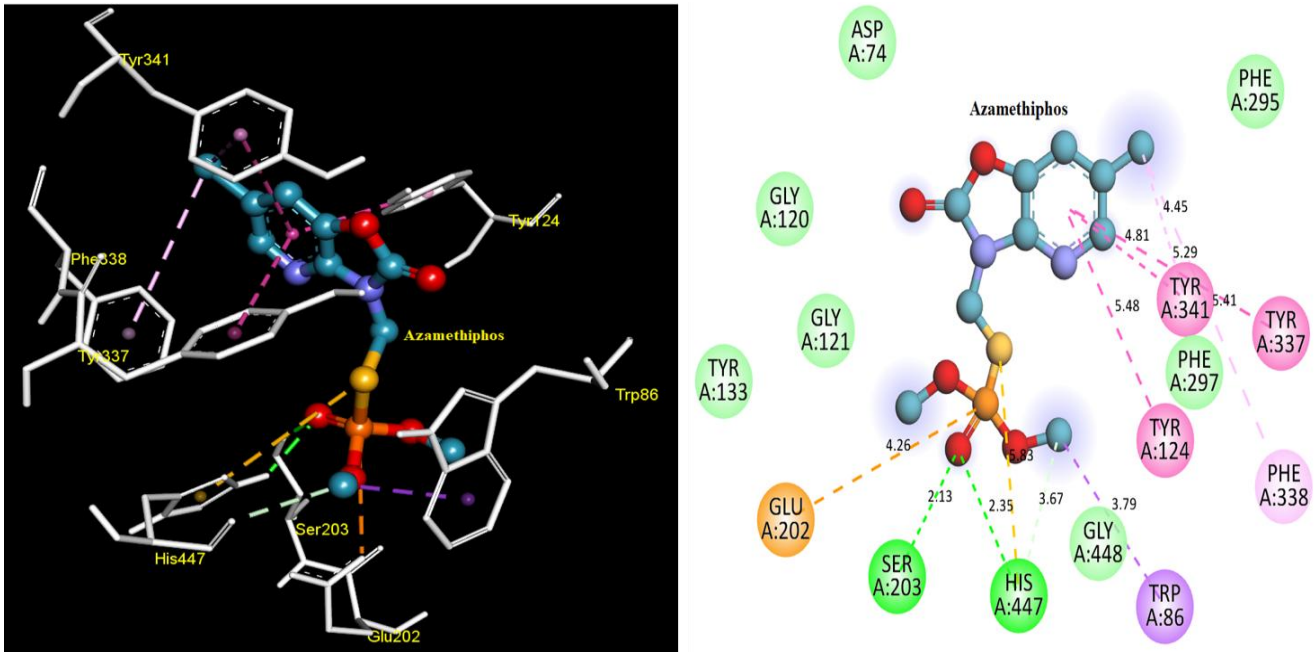

Figure 4: Interaction of Azamethiphos with hAChE active site: 3D structure of Azamethiphos-hAChE (left) and 2D structure (right) indicating types of interactions

3.2.4. Docking of Methylparathion into hAChE

The selected Methylparathion-hAChE complex (-6.4 Kcal/mol) stabilized via many types of interactions at the CAS catalytic triad (Ser203/His447/Glu202) and anionic subsite (Trp86). Methylparathion bound with Ser203 via a conventional hydrogen bond, His447 via a conventional hydrogen and carbon-hydrogen bonds, Glu202 via electrostatic interaction (attractive charge), and Trp86 via hydrophobic bonds (Pi-Sigma and Pi-Pi T-shaped). Furthermore, Methylparathion interacted with PAS amino acid residue at Phe338 via Pi-sulfur bond and with Tyr124 via conventional hydrogen bond (Table 2) & (Figure 5, left). Other amino acid residues became closer to the pesticide without interactions involving Gly120, Gly121, Tyr337, Tyr133, Asp74, Asn87, and Gly448 (Figure 5, right).

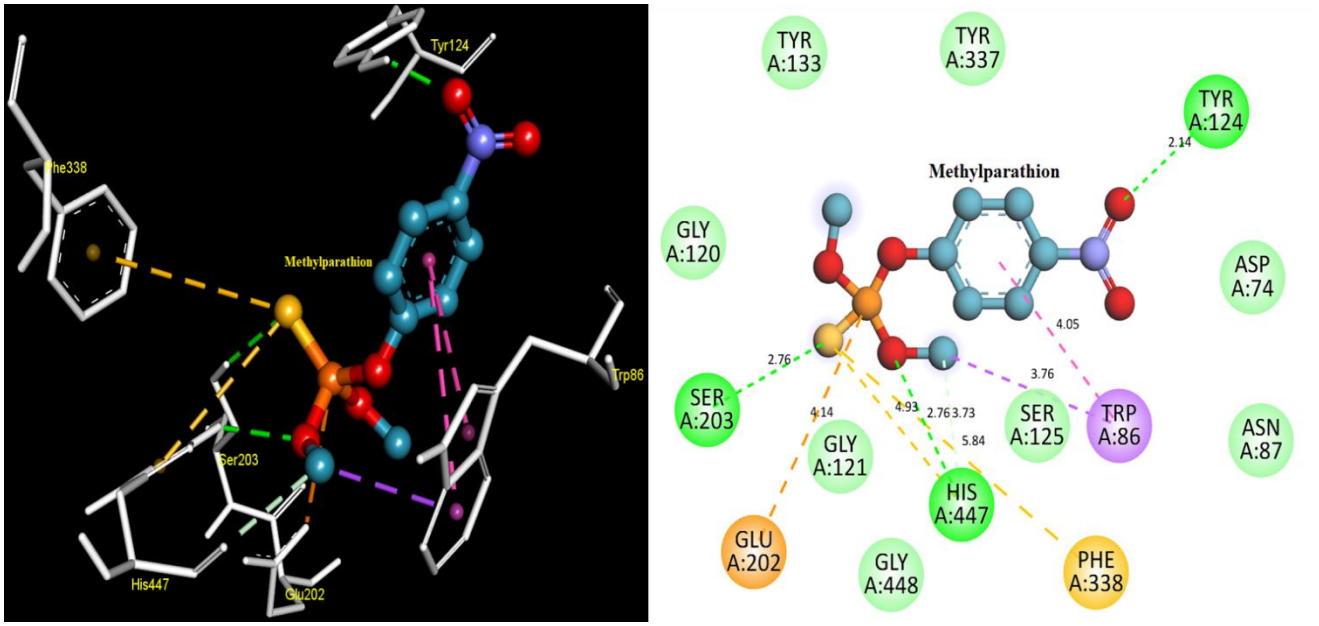

Figure 5: Interaction of Methylparathion with hAChE active site: 3D structure of Methylparathion-hAChE (left) and 2D structure (right) indicating types of interactions.

3.2.5. Docking of Malathion into hAChE

The selected Malathion-hAChE conformer (-6.4 Kcal/mol) stabilized via many types of interactions. Malathion interacted with the CAS catalytic triad at Ser203 via a conventional hydrogen bond, His447 via a conventional hydrogen bond as well as Pi-sulfur bond, and Glu202 via electrostatic interaction (attractive charge). Also, Malathion binds with PAS amino acid residues at Phe338 and Phe297 via two hydrophobic Pi-alkyl bonds (Table 2) & (Figure 6, left). Other amino acid residues became closer to the pesticide without interactions involving Trp86, Gly121, Tyr337, Asp74, Asn87, Gly448, and Ser125 (Figure 6, right).

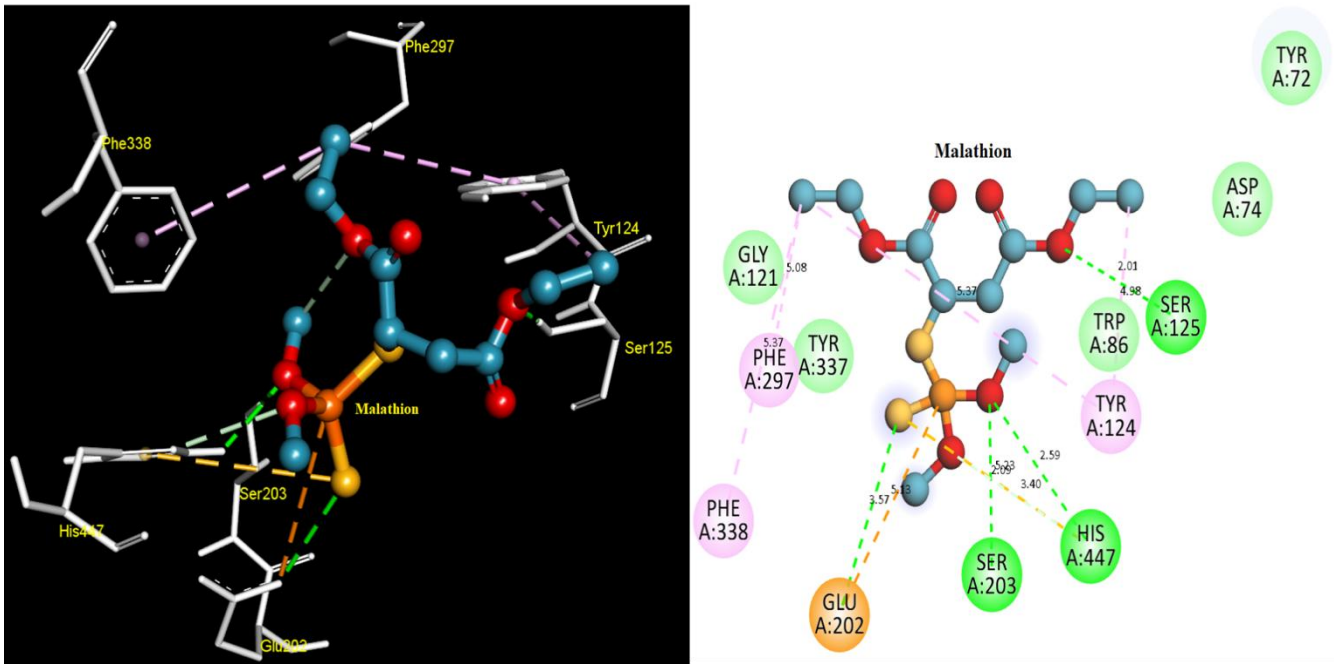

Figure 6: Interaction of Malathion with hAChE active site: 3D structure of Malathion-hAChE (left) and 2D structure (right) indicating types of interactions.

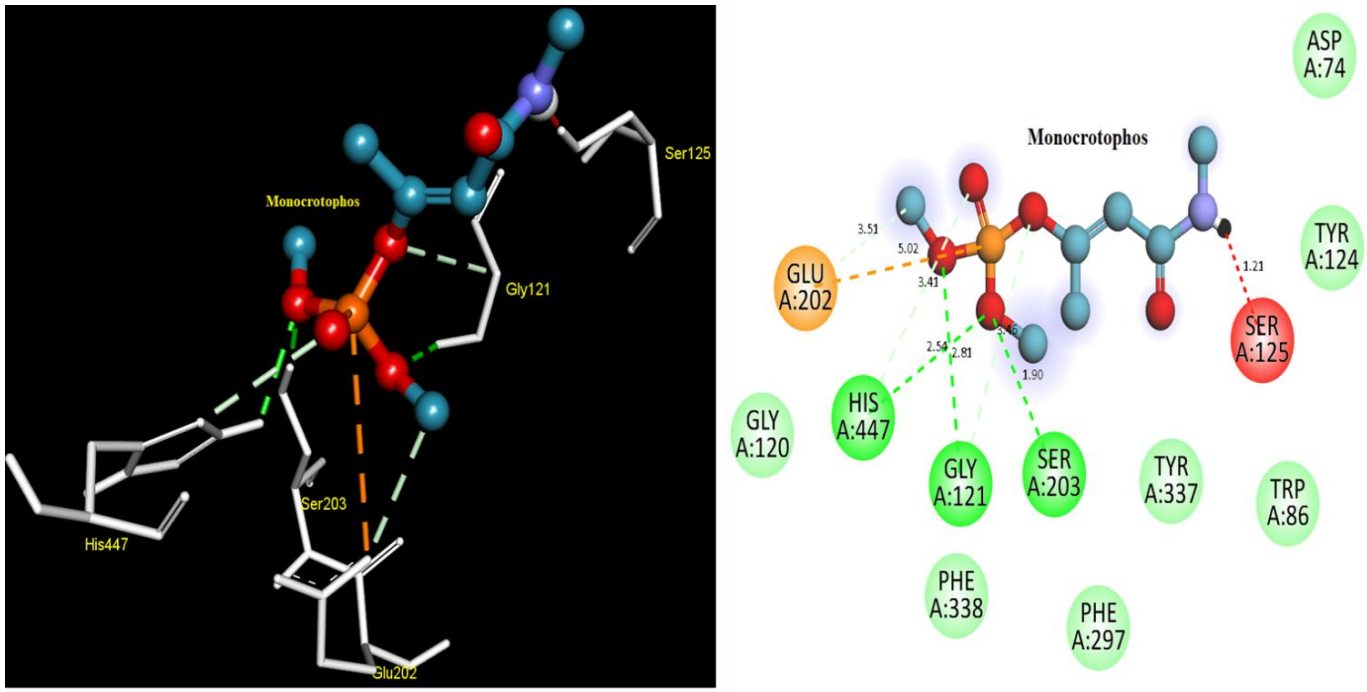

Figure 7: Interaction of Monocrotophos with hAChE active site: 3D structure of Monocrotophos-hAChE (left) and 2D structure (right) indicating types of interactions.

3.2.6. Docking of Monocrotophos into hAChE

The selected Monocrotophos-hAChE conformer (-6.1 Kcal/mol) stabilized via many types of interaction. Monocrotophos interacted with the CAS catalytic triad at Ser203 via a conventional hydrogen bond, His447 via a conventional hydrogen bond as well as a carbon-hydrogen bond, and Glu202 via an electrostatic interaction (attractive charge) and carbon-hydrogen bond. Monocrotophos binds with Gly121 (oxyanion hole) via conventional hydrogen and carbon-hydrogen bonds (Table 2) & (Figure 7, left). Moreover, an unfavorable interaction (donor-donor) was observed between Monocrotophos and Ser125, and other amino acid residues (Phe297, Phe338, Trp86, Gly120, Tyr337, Tyr124, and Asp74) became closer to the pesticide without interactions (Figure 7, right).

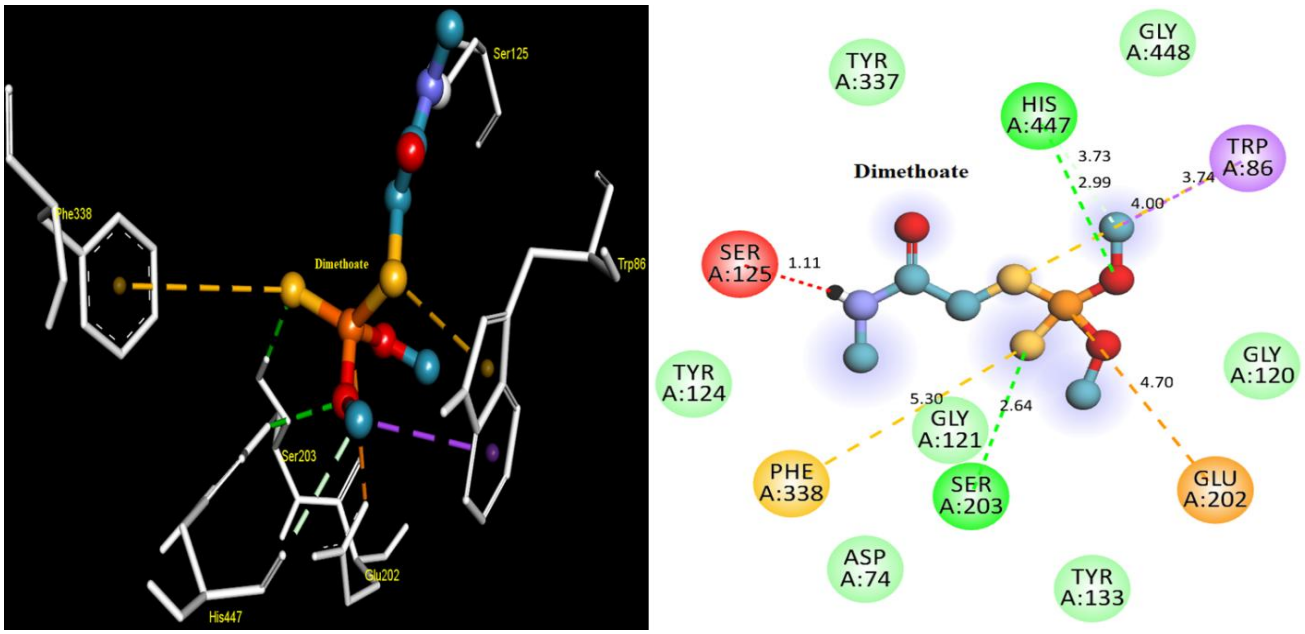

Figure 8: Interaction of Dimethoate with hAChE active site: 3D structure of Dimethoate-hAChE (left) and 2D structure (right) indicating types of interactions.

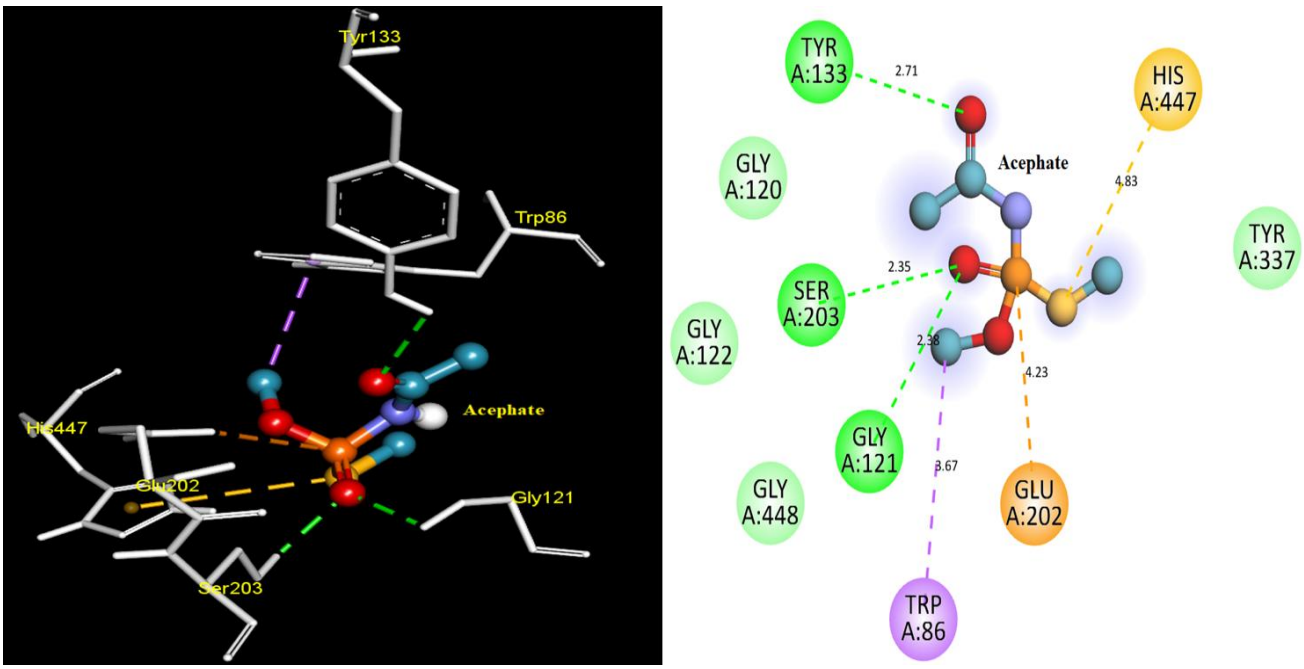

Figure 9: Interaction of Acephate with hAChE active site: 3D structure of Acephate-hAChE (left) and 2D structure (right) indicating types of interactions.

3.2.7. Docking of Dimethoate into hAChE

The selected Dimethoate-hAChE complex (-5.2 Kcal/mol) stabilized via many types of interaction at the CAS catalytic triad and anionic subsite (Trp86). In this respect, Dimethoate binds with Ser203 via a conventional hydrogen bond, His447 via a conventional hydrogen bond as well as carbon-hydrogen, and Glu202 via electrostatic interaction (attractive charge), as well as with Trp86 via hydrophobic bonds (Pi-Sigma) and Pi-sulfur bond. Dimethoate also interacted only with Phe338 in the PAS region via the Pi-sulfur bond (Table 2) & (Figure 8, left). On the other hand, an unfavorable interaction (donor-donor) between Dimethoate and Ser125 and other amino acid residues (Gly120, Gly121, Tyr133, Tyr337, Tyr124, Asp74, and Gly448) formed the pesticide without interactions (Figure 8, right).

3.2.8. Docking of Acephate into hAChE

The selected Acephate-hAChE conformer (-5.1 Kcal/mol) stabilized via many types of interaction. Acephate fully interacted with the CAS catalytic triad at Ser203 via a conventional hydrogen bond, His447 via a Pi-sulfur bond, and Glu202 via electrostatic interaction (attractive charge), as well as with anionic subsite (Trp86) via a hydrophobic bond (Pi-Sigma). Acephate also interacted with Gly121 and Tyr133 via conventional hydrogen bonds (Table 2) & (Figure 9, left). Other amino acid residues became closer to the Acephate without interactions involving Gly120, Gly122, Tyr337, and Gly448 (Figure 9, right).

3.3. Analysis of lowest energy conformers of OPs in the second group (interacted with His447, not Ser203)

3.3.1. Docking of Triazophos into AChE

The selected complex of Triazophos-hAChE (-7.9 Kcal/mol) stabilized via many types of interactions. Triazophos interacted with CAS at His447 (Pi-Alkyl), Trp86 (Pi-sigma), and an unfavorable interaction (Positive-Positive) was observed between the nitrogen of His447 and pesticide phosphorous. Triazophos also interacted with PAS amino acid residues at Tyr337 via hydrophobic bonds (Pi-Sigma), Phe338 via hydrophobic bonds (Pi-Pi T-shaped), Trp286 via hydrophobic bonds (Pi-Pi stacked), Tyr341 via hydrophobic bonds (Pi-Pi stacked), and Tyr124 via hydrophobic bonds (Pi-Pi T-shaped). Moreover, Triazophos interacted with Gly121 via a conventional hydrogen bond (Table 3) & (Figure 10, left). Other amino acid residues became closer to the pesticide without interactions involving Ser203, Phe295, Phe297, Val294, and Ser125 (Figure 10, right). Our results suggested that the proximity of Ser203 may convert this pesticide to be more toxic and an irreversible inhibitor via interaction with the residue at the CAS.

Table 3: Molecular docking results of OPs interacted with active site His447 not Ser203 of hAChE protein (6WUZ)

Name	Energy (kcal/mol)	Interactive amino acids
Triazophos	-7.9	HIS447, TRP86, GLY121, PHE338, TYR337, TYR124 TRP286 and TYR341
Azinphosmethyl	-7.7	HIS447, PHE295, TYR337, TYR124, TRP286 and TYR341
Quinalphos	-7.6	HIS447, TRP86, TYR337, TYR124, TRP286, TYR341 and ASP74
Chlorpyrifos	-7.0	HIS447, TRP86, PHE297, TYR337, TYR124, ASP74 and SER125
Parathion	-6.9	HIS447, TRP86, PHE295, TYR124 and TYR341
Fenthion	-6.4	HIS447, TYR124, TRP286, TYR341and TYR72
Cadusafos	-5.8	HIS447, TRP86, PHE297, PHE338, TYR337, TYR124 and SER125
Ethion	-5.6	HIS447, GLU202, TRP86, TYR337, TYR124, TYR341, ASP74 and THR83
Dichlorvos	-5.0	HIS447, TRP86, TYR337, TYR124, ASP74and SER125

3.3.2. Docking of Azinphosmethyl into hAChE

The selected conformer of Azinphosmethyl-hAChE (–7.7 Kcal/mol) stabilized via many types of interaction. Azinphosmethyl interacted with CAS at His447 via Pi-Sulfur interaction, while with PAS at Trp286 via two hydrophobic bonds (Pi-Pi Stacked), Tyr341 via two hydrophobic bonds (Pi-Pi Stacked), and Tyr337 via Pi-Sulfur interaction. The Azinphosmethyl formed a conventional hydrogen bond with Phe295 (Table 3) & (Figure 11, left). It also became closer to Ser203, Gly121, Gly122, Phe297, Phe338, Val294, Ser125, and Arg296 (Figure 11, right). The proximity of Ser203 may convert Azinphosmethyl to a more toxic and irreversible inhibitor via interaction with the residue at the CAS.

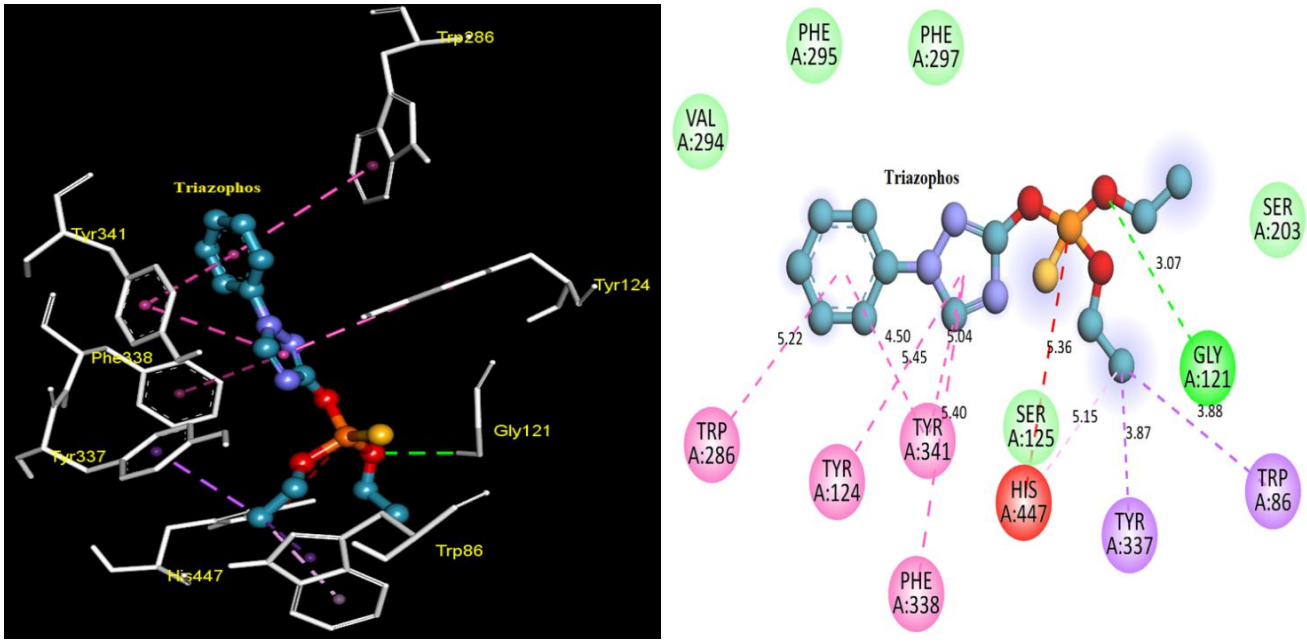

Figure 10: Interaction of Triazophos with hAChE active site: 3D structure of Triazophos-hAChE (left) and 2D structure (right) indicating types of interactions.

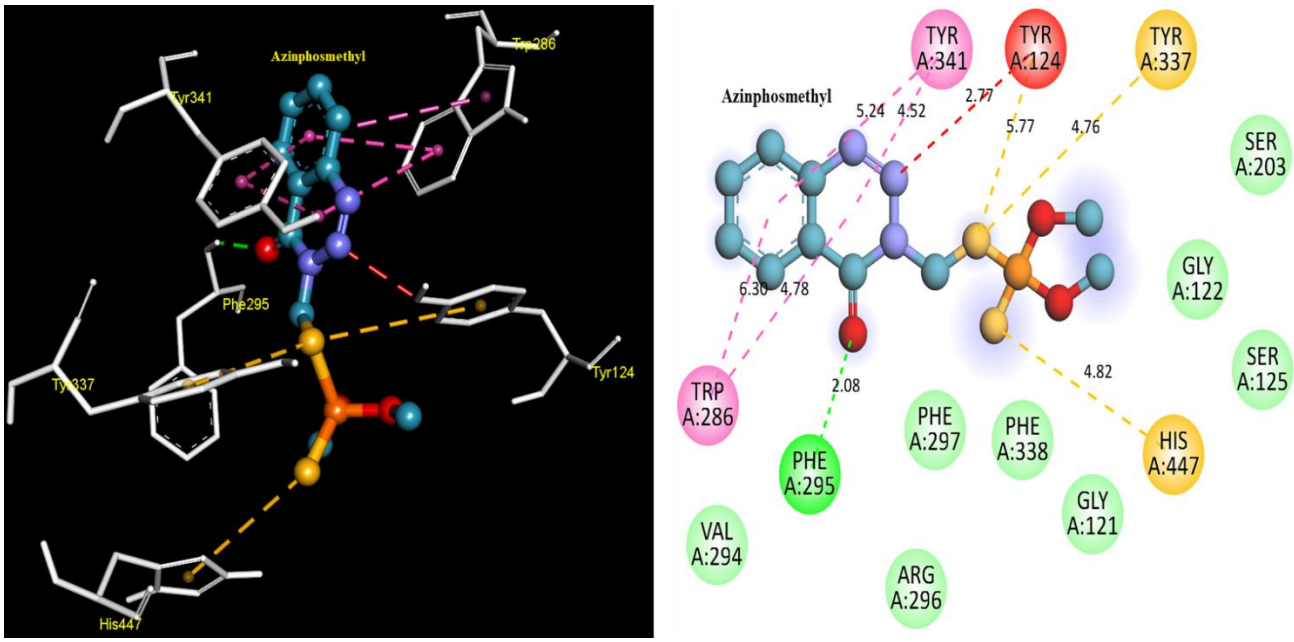

Figure 11: Interaction of Azinphosmethyl with hAChE active site: 3D structure of Azinphosmethyl-hAChE (left) and 2D structure (right) indicating types of interactions.

3.3.3. Docking of Quinalphos into hAChE

The selected Quinalphos-hAChE conformer (-7.6 Kcal/mol) stabilized via many types of interaction. Quinalphos interacted with CAS at His447 via a hydrophobic bond (Pi-Alkyl) and with Trp86 via hydrophobic bonds (Pi-Sigma). Quinalphos also interacted with PAS amino acid residues at Trp286 via a hydrophobic bond (Pi-Pi Stacked), Tyr341 via two hydrophobic bonds (Pi-Pi Stacked), Tyr124 via a conventional hydrogen bond as well as two hydrophobic (Pi-Pi T-shaped & Pi-alkyl) bonds, and Tyr337 via a hydrophobic bond (Pi-Alkyl). It also interacted with Asp74 via an electrostatic bond (an attractive charge) (Table 3) & (Figure 12, left), and became closer to Ser125 (Figure 12, right).

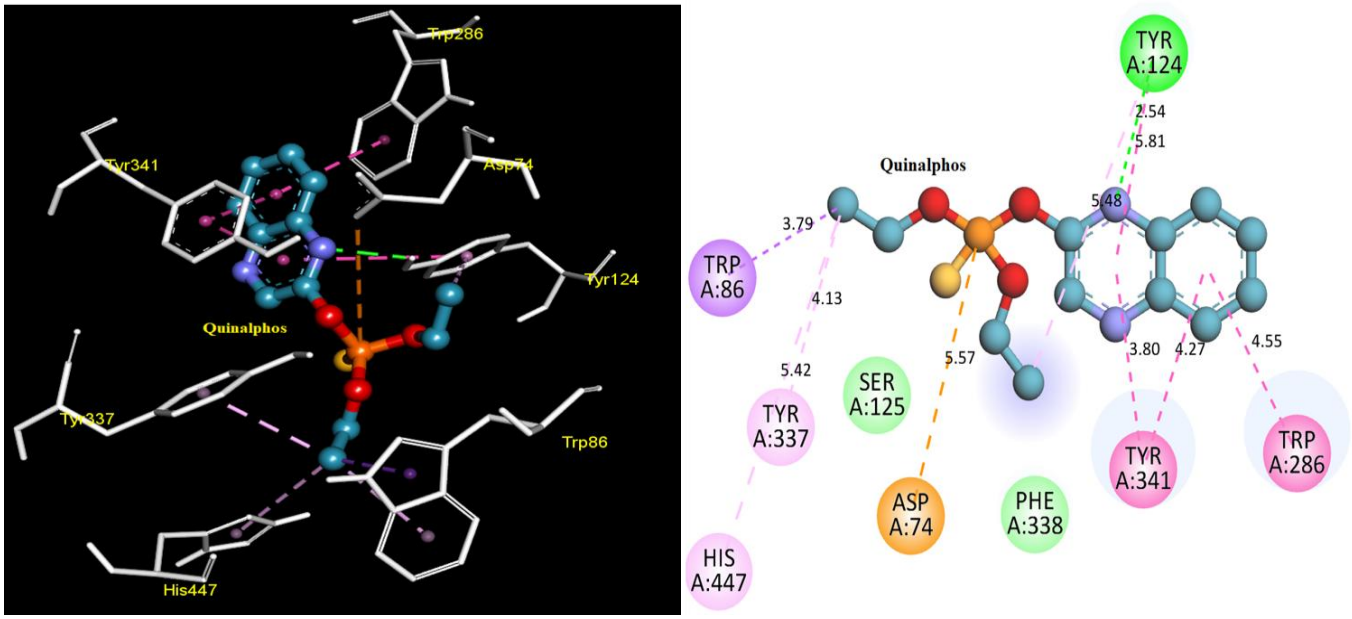

Figure 12: Interaction of Quinalphos with hAChE active site: 3D structure of Quinalphos-hAChE (left) and 2D structure (right) indicating types of interactions.

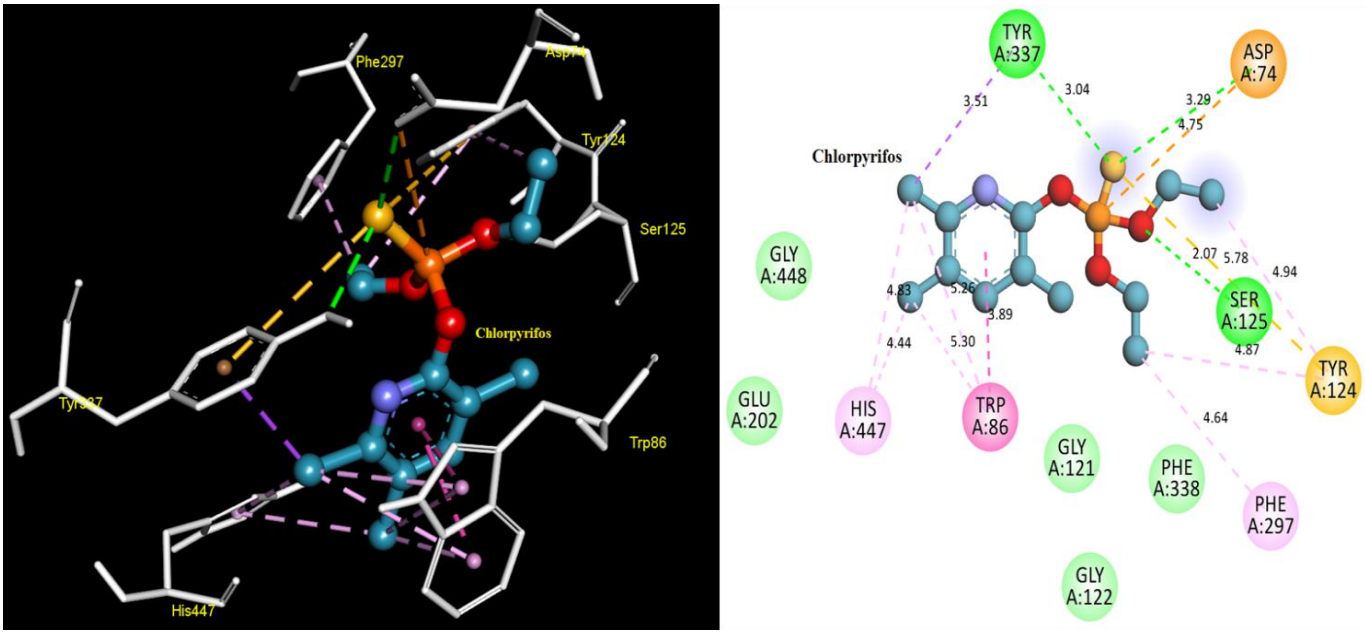

Figure 13: Interaction of Chlorpyrifos with hAChE active site: 3D structure of Chlorpyrifos-hAChE (left) and 2D structure (right) indicating types of interactions.

3.3.4. Docking of Chlorpyrifos into hAChE

The selected Chlorpyrifos-hAChE conformer (-7.0 Kcal/mol) stabilized via many types of interaction. Chlorpyrifos interacted with CAS at His447 via two hydrophobic bonds (Pi-Alkyl) and with Trp86 via three hydrophobic bonds (Pi-Pi Stacked & 2Pi-Alkyl). Chlorpyrifos also interacted with PAS amino acid residues at Tyr337 via a conventional hydrogen bond, hydrophobic bond (Pi-Sigma), and Pi-sulfur bond, as well as with Tyr124 via two hydrophobic (Pi-alkyl) bonds and Pi-sulfur bond. Furthermore, Chlorpyrifos formed a hydrophobic bond with Phe297 (Pi alkyl) and interacted with Asp74 via a conventional hydrogen bond as well as an electrostatic bond (attractive charge) (Table 3) & (Figure 13, left). While amino acid residues (Glu202, Phe338, Gly121, Gly122, Tyr133, Asn87, and Gly448) became closer to the pesticide without interactions (Figure 13, right).

3.3.5. Docking of Parathion into hAChE

The selected Parathion-hAChE conformer (-6.9 Kcal/mol) stabilized via many types of interaction. Parathion interacted with CAS at His447 via the Pi-sulfur bond and with Trp86 via the hydrophobic bond (Pi-Sigma). Parathion also interacted with PAS amino acid residues at Tyr337 via a carbon-hydrogen bond, Tyr124 via hydrophobic (Pi-Pi T-Shaped), and Tyr341 via a hydrophobic bond (Pi-Pi T-Shaped). Parathion also formed a conventional hydrogen bond with Phe295 (Table 3) & (Figure 14, left) and become closer to Phe297, Phe338, Gly121, Asp74, Val294, and Ser125 (Figure 14, right).

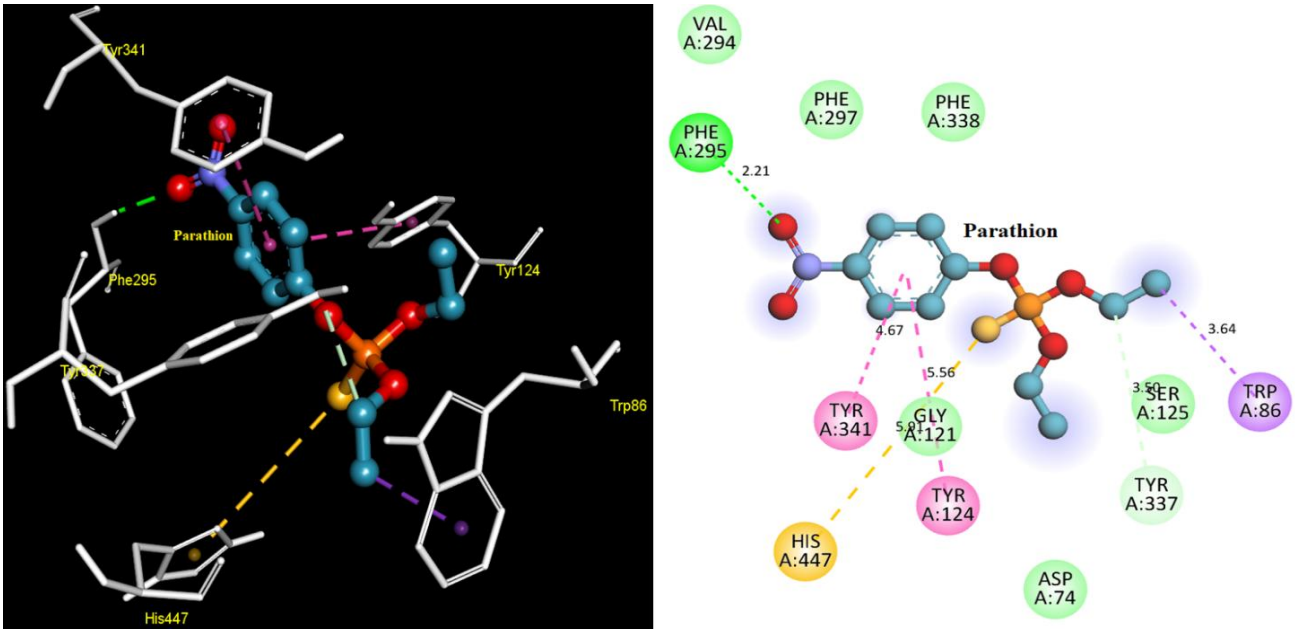

Figure 14: Interaction of Parathion with hAChE active site: 3D structure of Parathion-hAChE (left) and 2D structure (right) indicating types of interactions.

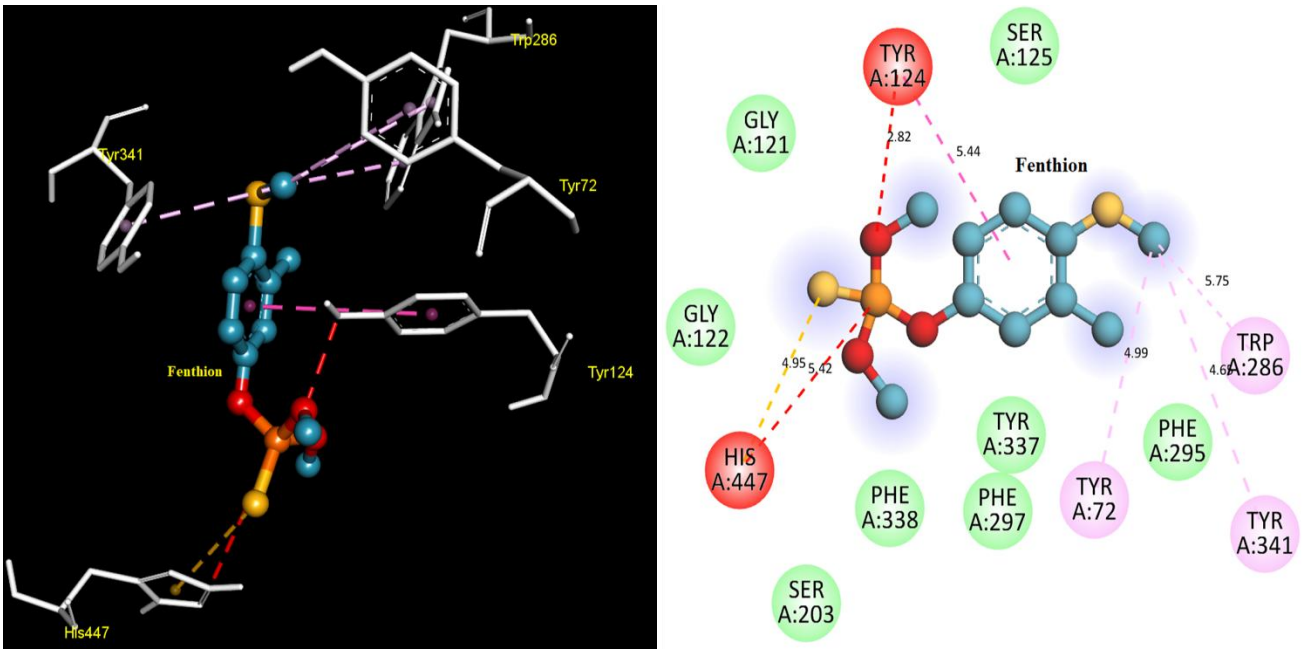

Figure 15: Interaction of Fenthion with hAChE active site: 3D structure of Fenthion-hAChE (left) and 2D structure (right) indicating types of interactions.

3.3.6. Docking of Fenthion into hAChE

The selected Fenthion-hAChE conformer (-6.4 Kcal/mol) stabilized via many types of interaction. Fenthion interacted with CAS at His447 via Pi-sulfur bond and unfavorable (positive –positive charge) interaction. It also interacted with PAS amino acid residues at Tyr124 via a hydrophobic (Pi-Pi T-Shaped), unfavorable (acceptor-acceptor) interaction from Tyr124 hydroxyl group to the oxygen of pesticide, Tyr341 via a hydrophobic bond (Pi-Alkyl), and Trp2861 via a hydrophobic bond (Pi-Alkyl). Fenthion also interacted with Tyr72 via a hydrophobic bond (Pi-Alkyl) (Table 3) & (Figure 15, left) and became closer to Ser203, Phe295, Phe297, Phe338, Gly121, Gly122, Tyr337, and Ser125 (Figure 15, right). The close proximity of Ser203 may convert this pesticide to be more toxic and an irreversible inhibitor via interaction with the residue at the CAS.

3.3.7. Docking of Cadusafos into hAChE

The selected Cadusafos-hAChE conformer (-5.8 Kcal/mol) stabilized via many types of interaction. Cadusafos interacted with CAS at His447 via a hydrophobic bond (Pi-Alkyl) and with Trp86 via three hydrophobic bonds (Pi-Alkyl & 2Pi-Sigma). Cadusafos also interacted with PAS amino acid residues at Phe338 via a hydrophobic bond (Pi-Alkyl), Tyr337 via a hydrophobic bond (Pi-Sigma) and Pi-sulfur bond, Tyr124 via a conventional hydrogen bond, and an unfavorable (acceptor-acceptor) from Tyr124 hydroxyl group to oxygen of pesticide. It also interacted with conventional hydrogen bonds with Ser125 (Table 3) & (Figure 16, left). While Ser203, Gly121, Gly122, Asn87, Asp74, and Gly448 amino acid residues became closer to the pesticide without interactions (Figure 16, right). The close proximity of Ser203 may convert this pesticide to be more toxic and an irreversible inhibitor via interaction with the residue at the CAS.

3.3.8. Docking of Ethion into hAChE

The selected Ethion-hAChE complex (-5.6 Kcal/mol) stabilized via many types of interaction. Ethion interacted with CAS at His447 via a conventional hydrogen bond and Pi-sulfur bond, Glu202 via an electrostatic (attractive charge) bond as well as a conventional hydrogen bond, and with Trp86 via an electrostatic (Pi-cation) bond, as well as a Pi-donor hydrogen bond. Ethion also interacted with PAS amino acid residues at Tyr337 via a conventional hydrogen and hydrophobic bond (Pi-Alkyl), Tyr124 via a conventional hydrogen bond. It also interacted with Thr83 via a conventional hydrogen bond (Table 3) & (Figure 17, left). While Ser203, Phe338, Gly120, Gly121, Gly122, Tyr133, Asp74, Asn87, Gly448, and Ser125 amino acid residues became closer to Ethion without interactions (Figure 17, right). The close proximity of Ser203 may convert this pesticide to a more toxic and irreversible inhibitor via interaction with the residue at the CAS.

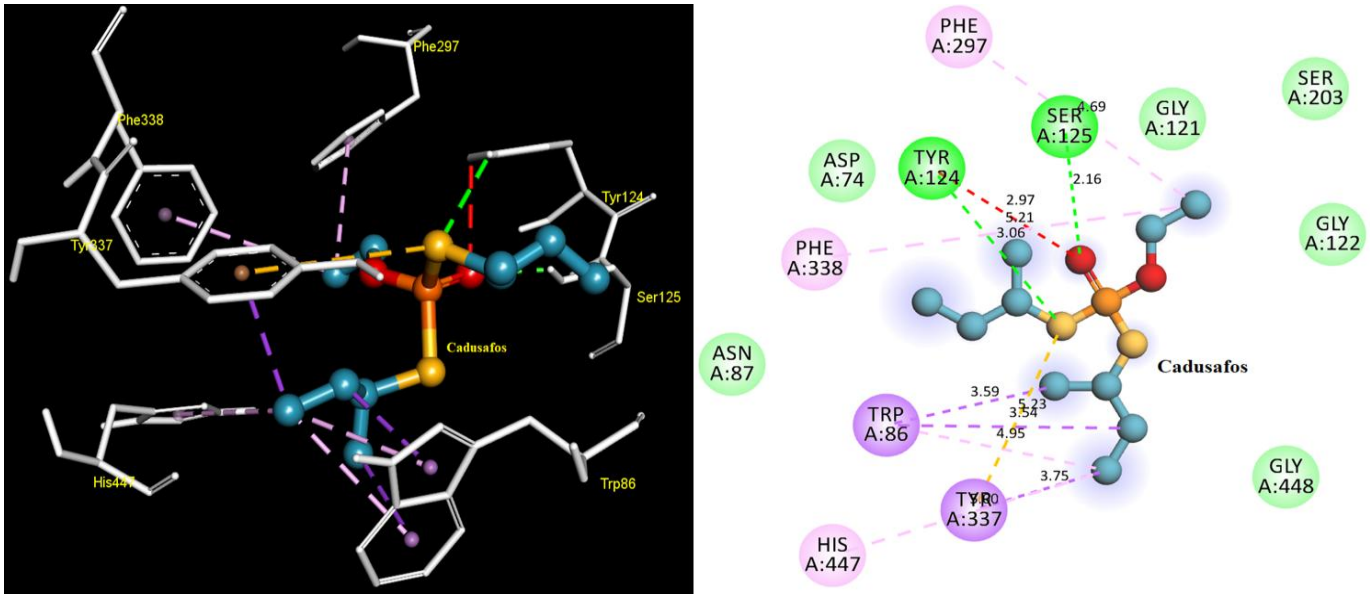

Figure 16: Interaction of Cadusafos with hAChE active site: 3D structure of Cadusafos-hAChE (left) and 2D structure (right) indicating types of interactions.

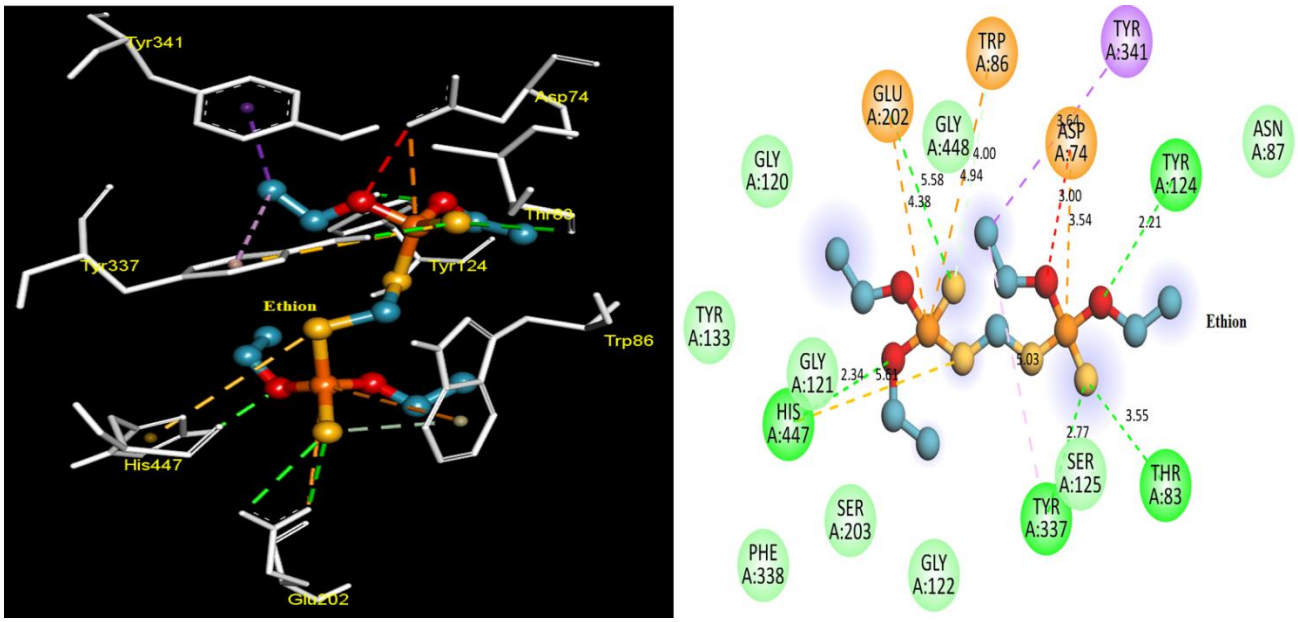

Figure 17: Interaction of Ethion with hAChE active site: 3D structure of Ethion-hAChE (left) and 2D structure (right) indicating types of interactions.

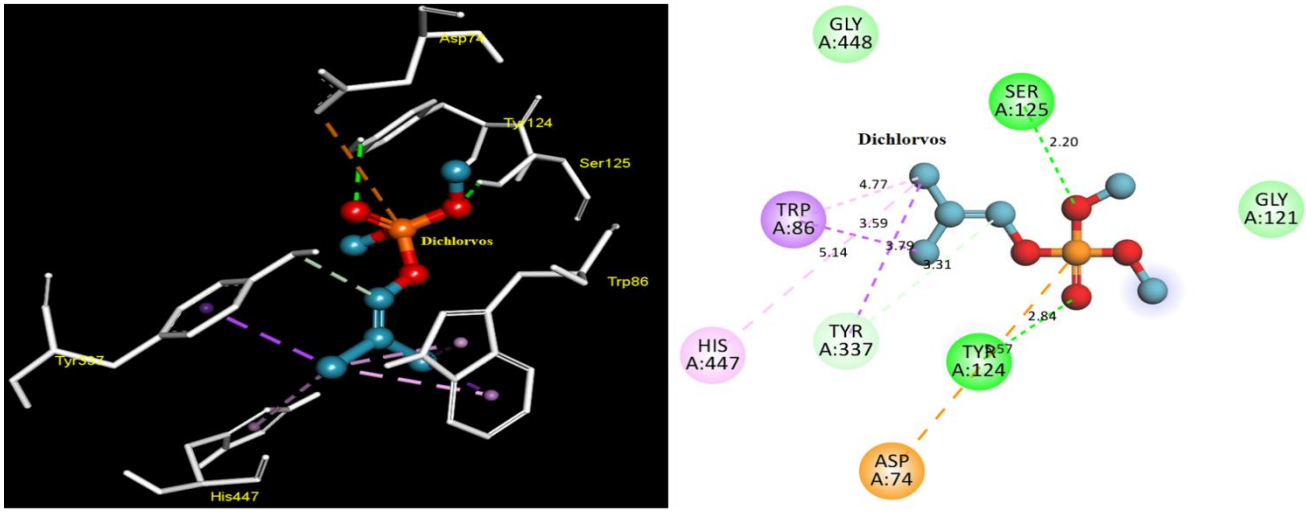

Figure 18: Interaction of Dichlorvos with hAChE active site: 3D structure of Dichlorvos-hAChE (left) and 2D structure (right) indicating types of interactions.

3.3.9. Docking of Dichlorvos into hAChE

The selected Dichlorvos-hAChE conformer (-5.0 Kcal/mol) stabilized via many types of interaction. Dichlorvos interacted with CAS at His447 via a hydrophobic bond (Pi-Alkyl) and with Trp86 via two hydrophobic bonds (Pi-Alkyl & Pi-Sigma). Dichlorvos also interacted with PAS amino acid residues at Tyr337 via a carbon-hydrogen bond as well as a hydrophobic bond (Pi-Sigma) and Tyr124 via a conventional hydrogen bond. It also interacted via conventional hydrogen bonds with Ser125 and Asp74 with an electrostatic bond (attractive charge) (Table 3 & Figure 18, left), and became closer to Gly121 and Gly448 (Figure 18, right).

3.4. Analysis of lowest energy conformers of OPs in the third group (not interacted with His447 or Ser203)

3.4.1. Docking of Phosmet into hAChE

The selected Phosmet-hAChE conformer (-7.5 Kcal/mol) stabilized via many types of interaction. Phosmet interacted with PAS amino acid residues at Phe338 via a Pi-sulfur bond, Tyr337 via a conventional hydrogen bond, Tyr124 via a conventional hydrogen bond, hydrophobic bond (Pi-Pi T-shaped), and Pi-Sulfur interaction, Tyr241 via two hydrophobic bonds (Pi-Pi T-shaped & Pi-Pi Stacked), and

Trp286 via two hydrophobic bonds (Pi-Pi Stacked). It also interacted with acyl pocket amino acids via a conventional hydrogen bond with Phe295 and Pi-Sulfur interactions with Phe297 (Table 4) & (Figure 19, left) and became closer to His447, Ser203, Gly121, Gly122, Asp74, and Val294 (Figure 19, right). These results suggested that the closed proximity of Ser203 and His447 from the catalytic triad, as well as Gly121 and Gly122 from the oxyanion hole, may convert Phosmet to a toxic and irreversible inhibitor via interaction with the enzyme CAS, especially with its low binding energy.

Table 4: Molecular docking results of Ops interacted with active site neither His447 nor Ser203 of hAChE protein (6WUZ)

Name	Energy (kcal/mol)	Interactive amino acids
Phosmet	-7.5	PHE295, PHE297, PHE338, TYR337, TYR124, TRP286 and TYR341
Coumaphos	-7.1	PHE295, TRP286, TYR341 and VAL294
Fenamiphos	-6.9	TYR337, TYR124, TRP286, TYR341 and TYR 72
Fenitrothion	-6.6	PHE295, TRP286, TYR341 and ARG296
Diazinon	-6.4	TYR124, TRP286, TYR341, SER293, LEU76 and TYR72
Dicrotophos	-6.2	GLU202, TRP86, TYR124, ASP74, THR83 and SER125
Profenofos	-6.0	TRP286, TYR341, TYR72, LEU76 and LEU289,
Naled	-5.9	TRP86, GLY121, TYR337, TYR124 and SER125
Chlorpyrifos-methyl	-5.6	PHE295, TRP286, TYR341and VAL294
Ethoprophos	-5.3	TRP86, GLY121, TYR337, TYR124 and SER125
Phosphamidon	-5.0	HIS381, ASP400 and ARG525
Phorate	-4.8	TRP86, PHE297, PHE338, TYR337, TYR124 and TYR341
Terbufos	-4.5	TRP286, TYR341, GLU292 and LEU289

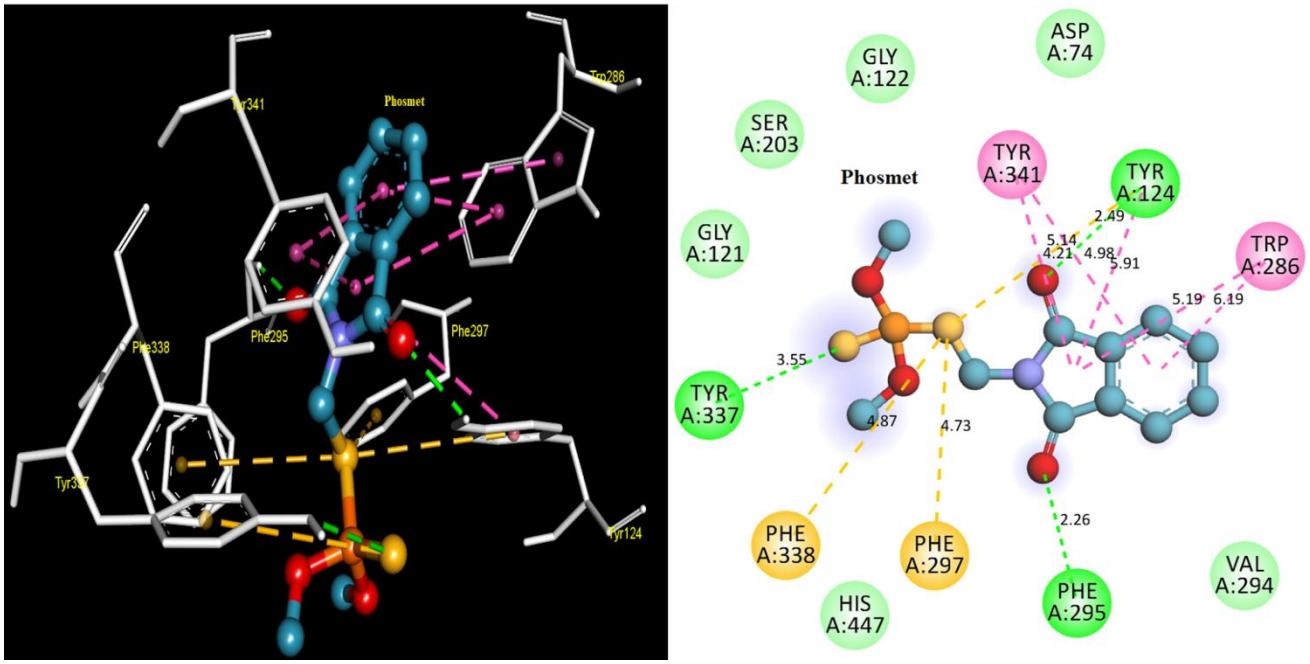

Figure 19: Interaction of Phosmet with hAChE active site: 3D structure of Phosmet-hAChE (left) and 2D structure (right) indicating types of interactions.

3.4.2. Docking of Coumaphos into hAChE

The selected Coumaphos-hAChE conformer (-7.1 Kcal/mol) stabilized via many types of interaction. Coumaphos interacted with PAS amino acid residues at Tyr341 via three hydrophobic (Pi-sigma & 2Pi-Pi Stacked) bonds and Trp286 that interacted with two

hydrophobic bonds (Pi-Pi Stacked) as well as an electrostatic (Pi-Cation) bond. Coumaphos also interacted with Phe295 via a conventional hydrogen bond and Val294 via a carbon-hydrogen bond (Table 4) & (Figure 20, left) and become closer to Phe297, Phe338, Tyr124, Tyr72, Ser293, Arg296, and Leu76 (Figure 20, right). These bonds might make Coumaphos a good hAChE reversible inhibitor as it mostly interacts with PAS amino acids and have higher probability to bind with those amino acids without any proximity to Ser203 and His447.

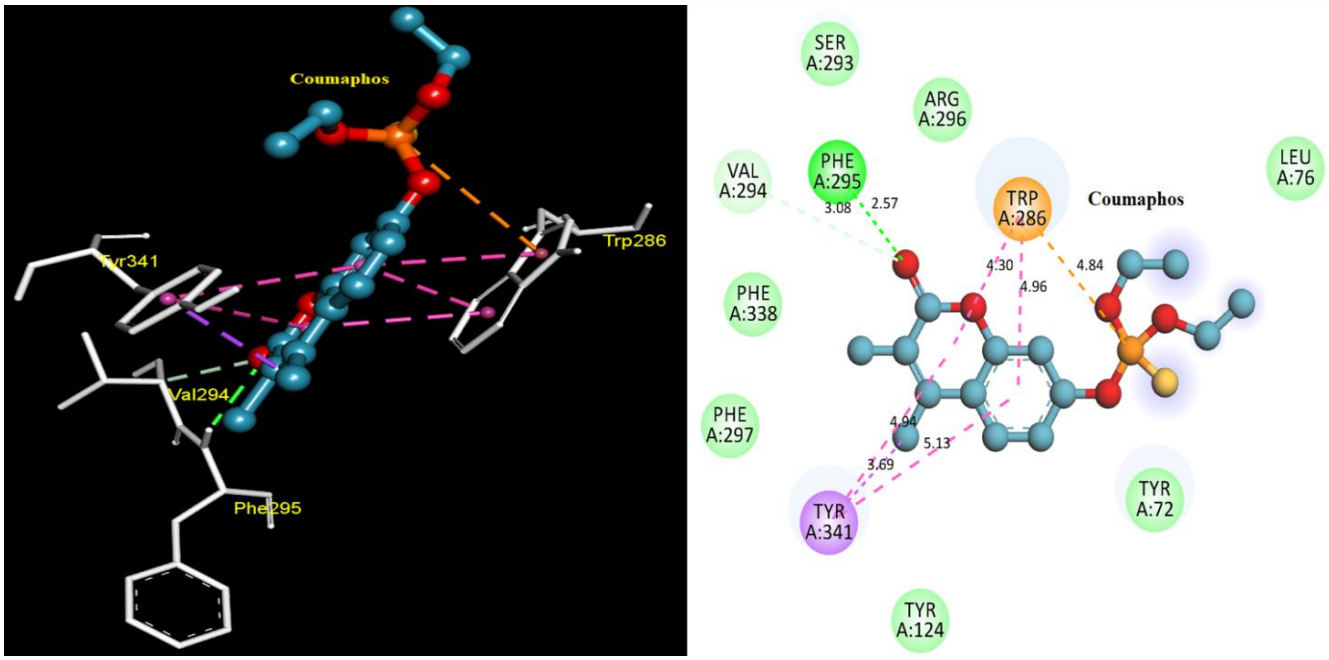

Figure 20: Interaction of Coumaphos with hAChE active site: 3D structure of Coumaphos-hAChE (left) and 2D structure (right) indicating types of interactions.

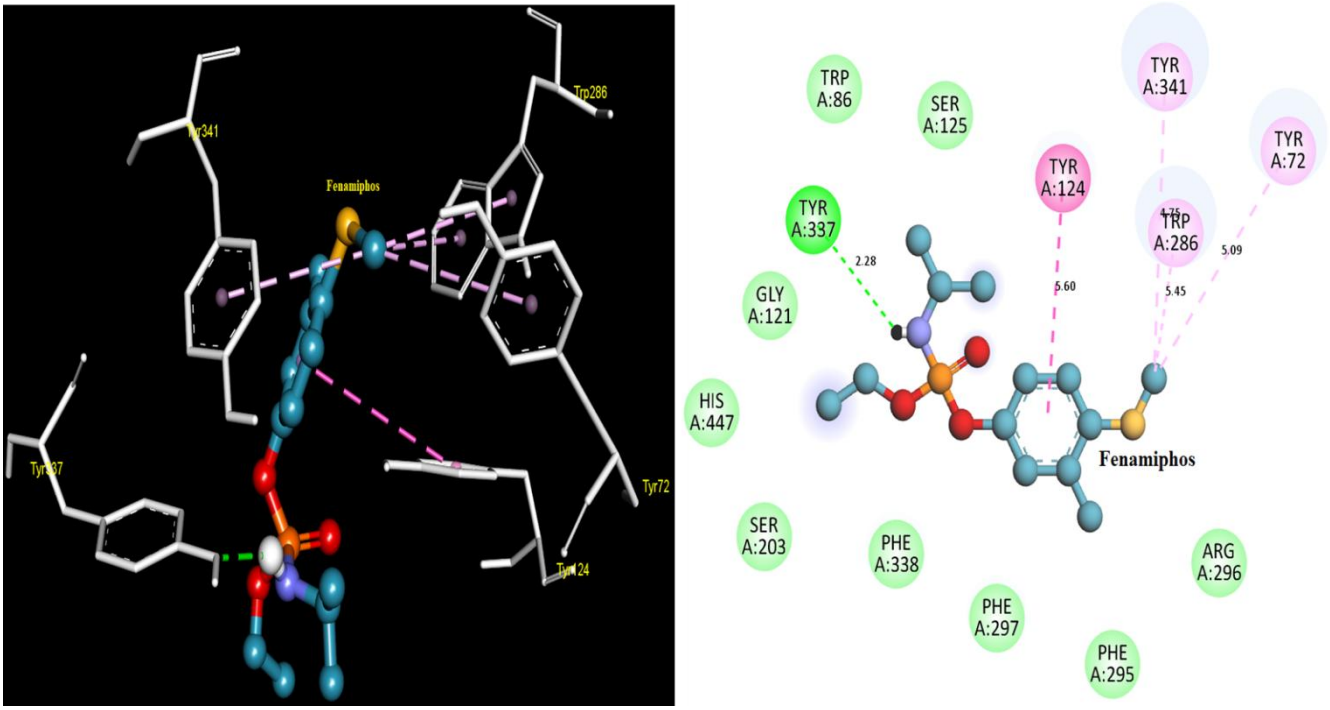

Figure 21: Interaction of Fenamiphos with hAChE active site: 3D structure of Fenamiphos-hAChE (left) and 2D structure (right) indicating types of interactions.

3.4.3. Docking of Fenamiphos into hAChE

The selected Fenamiphos-hAChE complex (-6.9 Kcal/mol) stabilized via many types of interaction. Fenamiphos interacted with PAS amino acid residues at Tyr337 via a conventional hydrogen bond, Tyr124 via a hydrophobic bond (Pi-Pi Stacked), Tyr241 via a hydrophobic bond (Pi-Alkyl), and Trp286 via a hydrophobic bond (Pi-Alkyl). Fenamiphos also interacted with Tyr72 via a hydrophobic bond (Pi-Alkyl) (Table 4 & Figure 21, left) and became closer to His447, Ser203, Phe295, Phe297, Phe338, Trp86, Gly121, Arg296, and Ser125 (Figure 21, right). The closed proximity to the catalytic triad (Ser203 and His447), acyl pocket (Phe295 and Phe297), and oxyanion hole (Gly121) may convert this pesticide to a more toxic and irreversible inhibitor via interaction with the enzyme CAS, especially with its low binding energy.

3.4.4. Docking of Fenitrothion into hAChE

The selected Fenitrothion-hAChE conformer (-6.6 Kcal/mol) stabilized via many types of interaction. Fenitrothion interacted with PAS amino acid residues at Tyr341 via a carbon-hydrogen bond as well as a hydrophobic (Pi-Pi Stacked) bond and Trp286 via two hydrophobic bonds (Pi-Pi Stacked). Fenitrothion also interacted with Phe295 and Arg296 via a conventional hydrogen bonds (Table 4) & (Figure 22, left) and become closer to Phe297, Phe338, Tyr124, Val294, Arg296, Leu76, Tyr72, and Thr75 (Figure 22, right). These findings suggested that Fenitrothion might be a good hAChE reversible inhibitor as it mostly interacted with PAS amino acids, and it has a higher probability to interact with those amino acids with no proximity of Ser203 and His447.

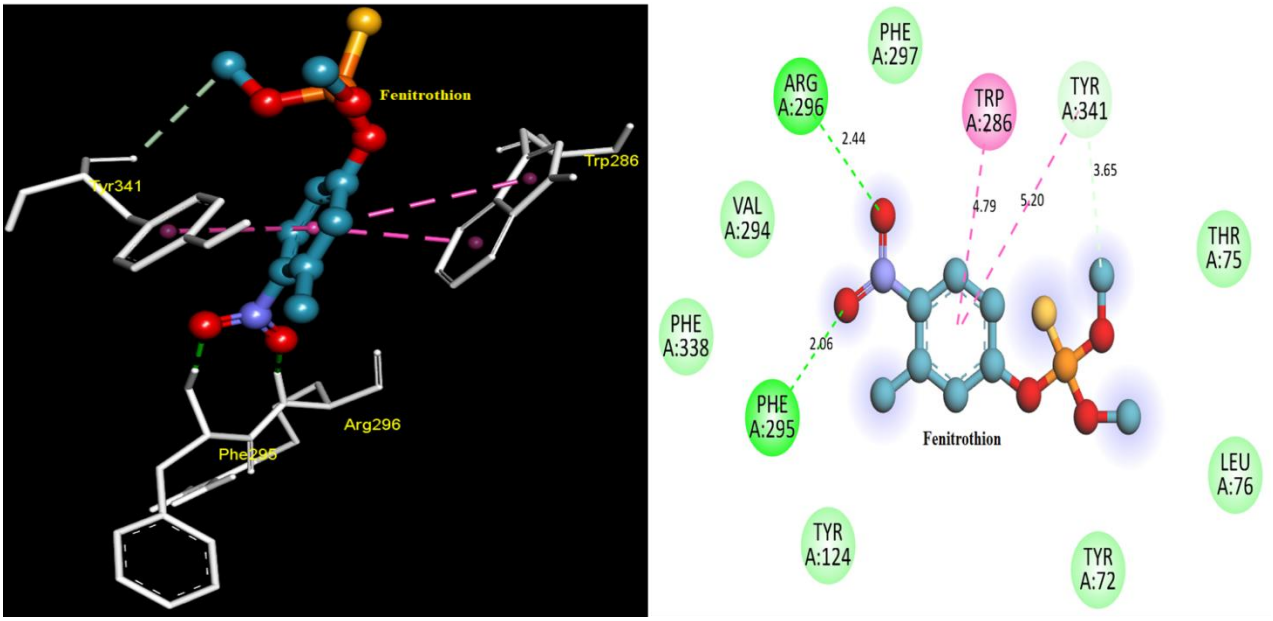

Figure 22: Interaction of Fenitrothion with hAChE active site: 3D structure of Fenitrothion-hAChE (left) and 2D structure (right) indicating types of interactions.

3.4.5. Docking of Diazinon into hAChE

The selected Diazinon-hAChE conformer (-6.4 Kcal/mol) stabilized via many types of interaction. Diazinon interacted with PAS amino acid residues at Tyr124 via a hydrophobic (Pi-Alkyl) bond, Tyr341 via three hydrophobic bonds (Pi-Pi Stacked & 2Pi-Alkyl), and Trp286 via electrostatic (Pi-Cation), Pi-Donor Hydrogen (Pi-Sulfur), and three hydrophobic (Pi-Pi Stacked) bonds. Diazinon also interacted with Ser293 via a carbon-hydrogen bond, Tyr72 via a hydrophobic bond (Pi-Alkyl), and Leu76 via a hydrophobic (Alkyl) bond (Table 4 & Figure 23, left). Moreover, it is close to Phe295, Phe297, Phe338, Tyr337, Val294, and Asp74 (Figure 23, right). These interactions suggested that Diazinon might be a good hAChE reversible inhibitor as it mostly interacted with PAS amino acids with a higher probability and no proximity to Ser203 and His447.

3.4.6. Docking of Dicrotofos into hAChE

The selected Dicrotofos-hAChE conformer (-6.4 Kcal/mol) stabilized via many types of interaction. Dicrotofos interacted with CAS at Glu202 via a carbon-hydrogen bond and with Trp86 via two hydrophobic bonds (Pi-Sigma). Dicrotofos also interacted with Tyr124

from the PAS region via a conventional hydrogen bond. It also interacted with Ser125 via a conventional hydrogen bond, Thr83 with a carbon-hydrogen bond, and Asp74 via an electrostatic bond (attractive charge) (Table 4 & Figure 24, left), and became closer to His447, Gly121, Tyr337, Tyr72, and Gly448 (Figure 24, right). The close proximity of His447 from the catalytic triad and Gly121 from oxyanion might increase the toxicity of Dicrotofos.

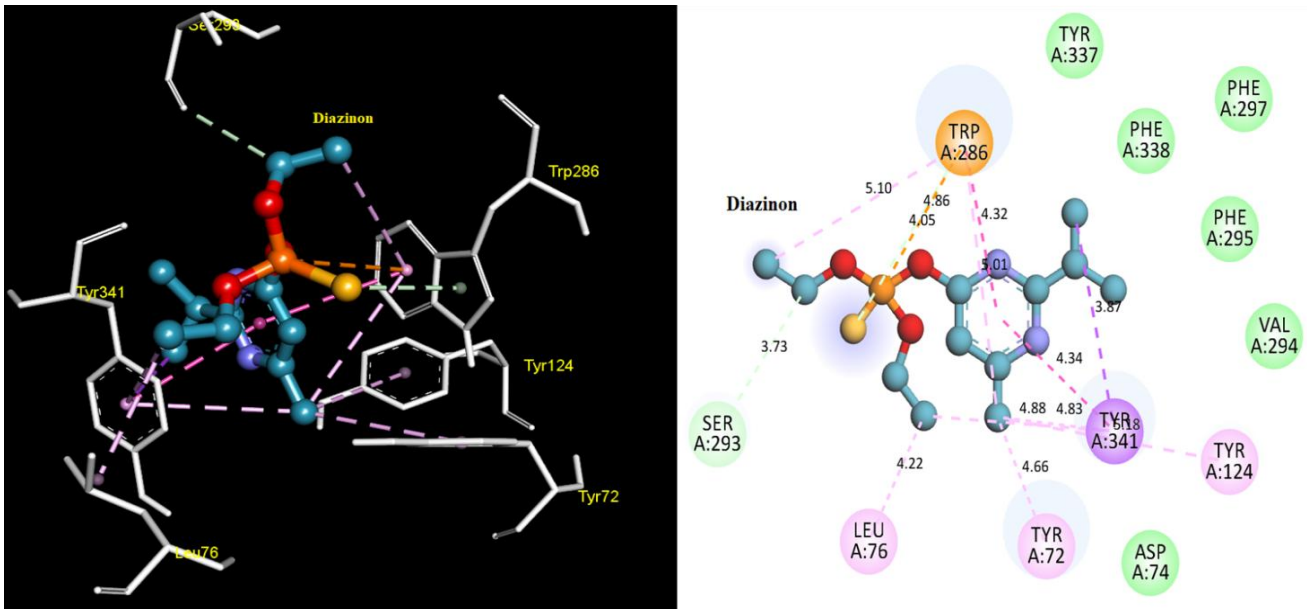

Figure 23: Interaction of Diazinon with hAChE active site: 3D structure of Diazinon-hAChE (left) and 2D structure (right) indicating types of interactions.

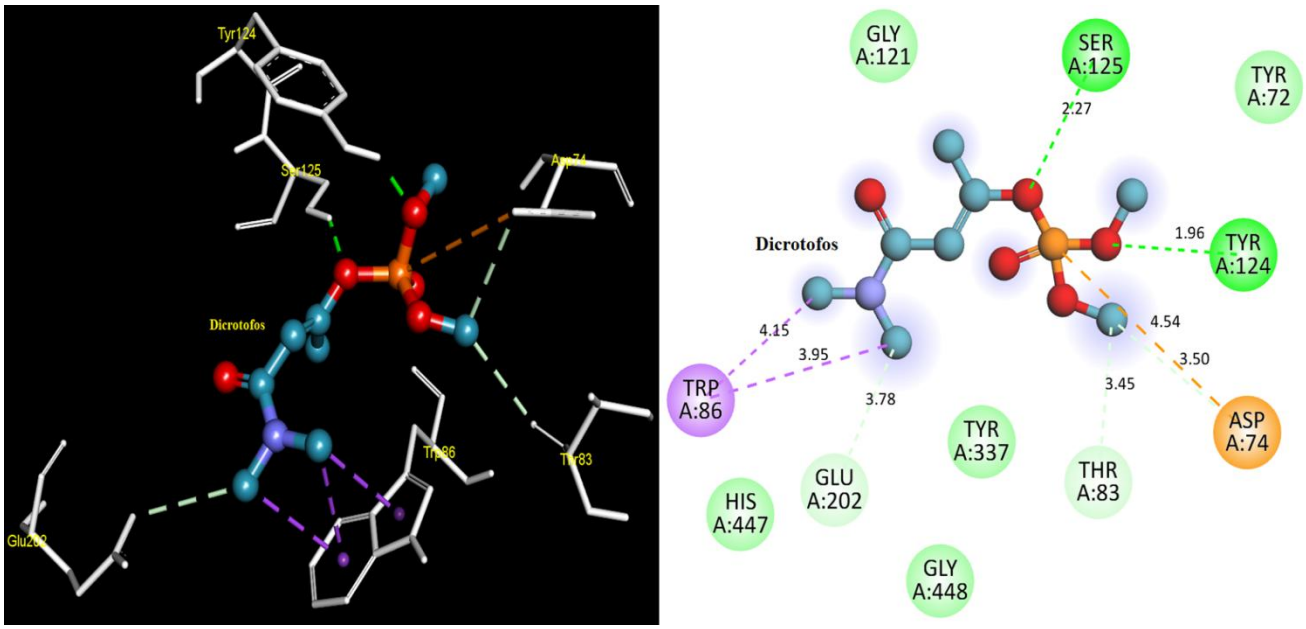

Figure 24: Interaction of Dicrotofos with hAChE active site: 3D structure of Dicrotofos-hAChE (left) and 2D structure (right) indicating types of interactions.

3.4.7. Docking of Profenofos into hAChE

The selected Profenofos-hAChE conformer (-6.0 Kcal/mol) stabilized via many types of interaction. Profenofos interacted with PAS amino acid residues at Tyr341 via two hydrophobic (Pi-Pi Stacked & Pi-Alkyl) bonds and Trp286 via an electrostatic (Pi-Cation) bond, besides two hydrophobic bonds (Pi-Pi Stacked & Pi-Alkyl). Profenofos also interacted with Tyr72 via a conventional hydrogen bond,

Leu289 via a hydrophobic bond (Alkyl), and Leu76 via a hydrophobic (Alkyl) bond (Table 4 & Figure 25, left), and became closer to Tyr124 (Figure 25, right). These interactions suggested that Profenofos might be a good hAChE reversible inhibitor as it has the highest probability to interact with PAS amino acids without any proximity to Ser203 and His447.

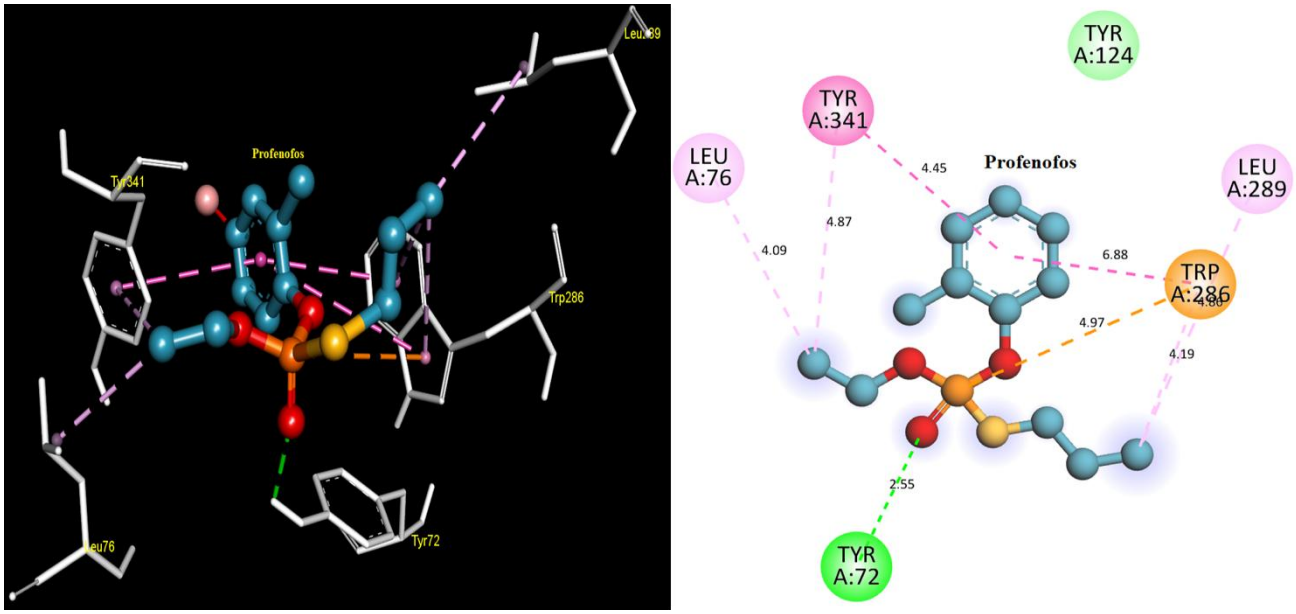

Figure 25: Interaction of Profenofos with hAChE active site: 3D structure of Profenofos-hAChE (left) and 2D structure (right) indicating types of interactions.

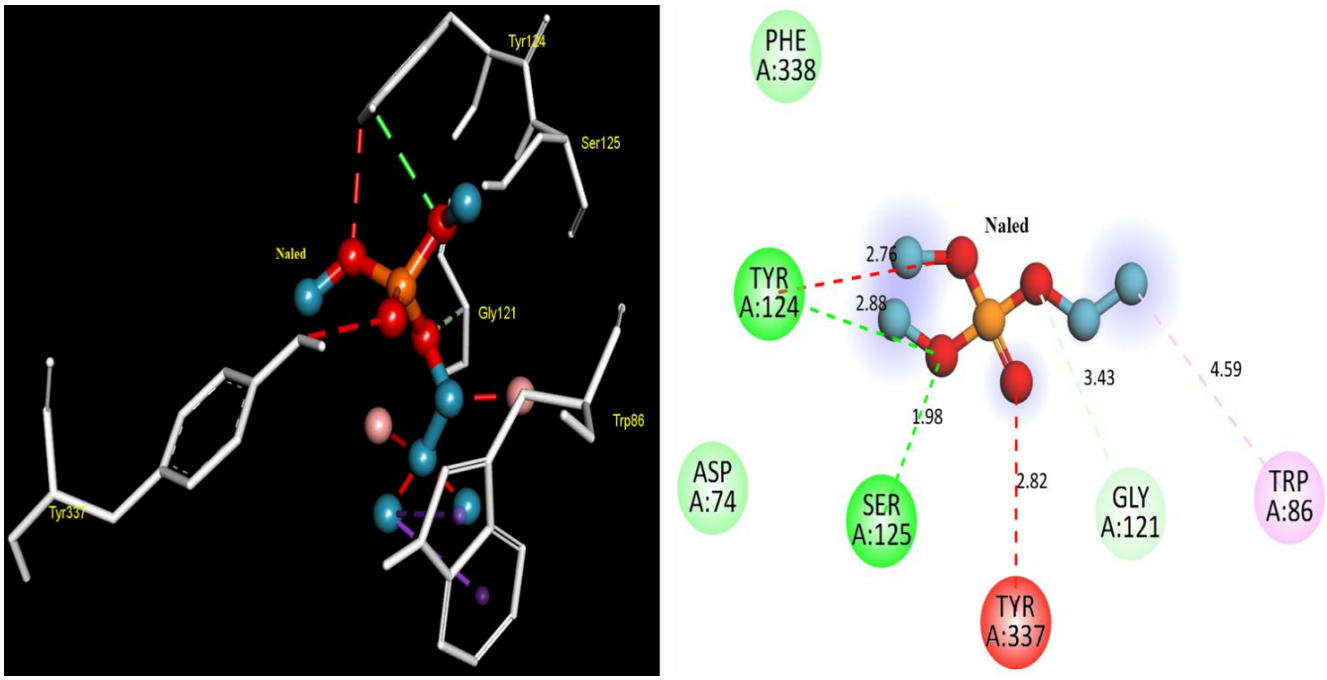

Figure 26: Interaction of Naled with hAChE active site: 3D structure of Naled-hAChE (left) and 2D structure (right) indicating types of interactions.

3.4.8. Docking of Naled into hAChE

The selected Naled-hAChE complex (-5.9 Kcal/mol) stabilized via many types of interaction. Naled interacted with Trp86 via two hydrophobic bonds (Pi-Alkyl) and Gly121 via a carbon-hydrogen bond. Naled also interacted with PAS amino acid residues at Tyr337 via an unfavorable interaction (Acceptor-Acceptor) and Tyr124 via a conventional hydrogen bond (H-donor), as well as an unfavorable

interaction (Acceptor-Acceptor). Furthermore, it interacted with Ser125 via a conventional hydrogen bond (H-donor) (Table 4 & Figure 26, left) and became closer to Phe338 and Asp74 (Figure 26, right).

3.4.9. Docking of Chlorpyrifos-methyl into hAChE

The selected Chlorpyrifos-methyl-hAChE conformer (-5.6 Kcal/mol) stabilized via many types of interaction. Chlorpyrifos-methyl interacted with PAS amino acid residues at Tyr341 via Pi-sulfur, besides two hydrophobic (Pi-Sigma & Pi-Pi-Stacked) bonds and Trp286 via two hydrophobic bonds (Pi-Pi Stacked). Chlorpyrifos also interacted with Phe297 via a hydrophobic bond (Pi-Alkyl) (Table 4 & Figure 27, left) and became closer to Phe295, Phe338, Leu76, Tyr72, Thr75, and Tyr124 (Figure 27, right). These results proposed that Chlorpyrifos-methyl might be a good hAChE reversible inhibitor as it mostly interacted with PAS amino acids with a higher probability, with no closed proximity to Ser203 and His447.

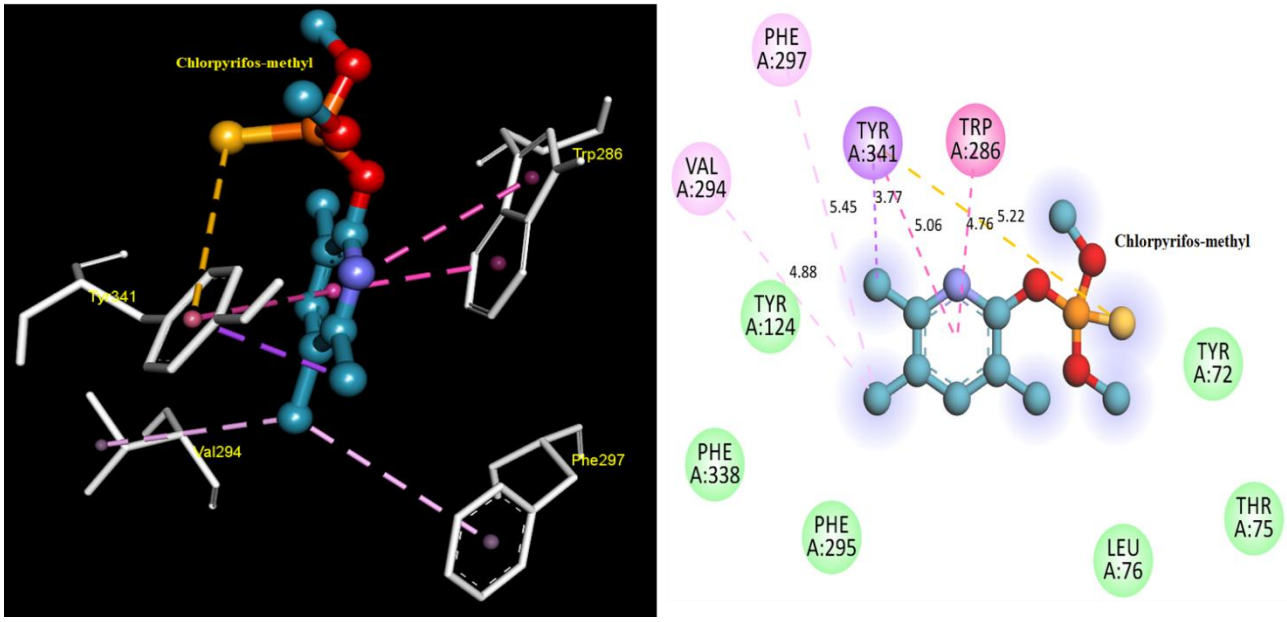

Figure 27: Interaction of Chlorpyrifos-methyl with hAChE active site: 3D structure of Chlorpyrifos-methyl-hAChE (left) and 2D structure (right) indicating types of interactions.

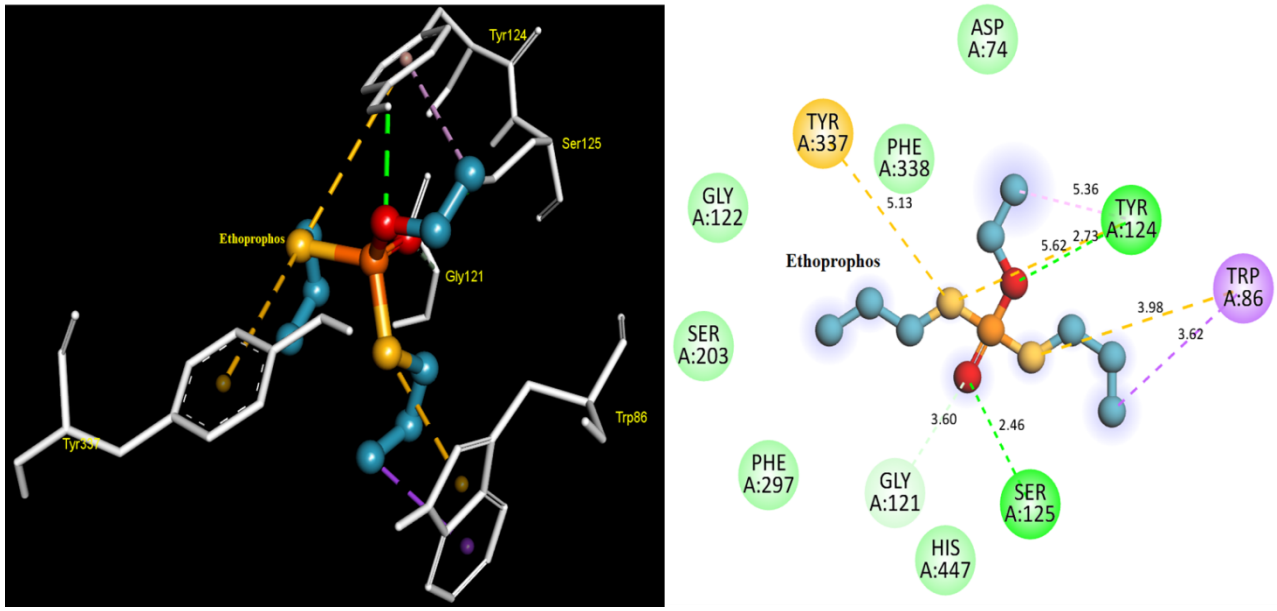

Figure 28: Interaction of Ethoprophos with hAChE active site: 3D structure of Ethoprophos-hAChE (left) and 2D structure (right) indicating types of interactions.

3.4.10. Docking of Ethoprophos into hAChE

The selected Ethoprophos-hAChE conformer (-5.3 Kcal/mol) stabilized via many types of interaction. Ethoprophos interacted with Trp86 via hydrophobic (Pi-sigma) as well as Pi-sulfur bond and Gly121 via a carbon-hydrogen bond. Ethoprophos also interacted with PAS amino acid residues at Tyr337 via a Pi-sulfur bond and Tyr124 via a conventional hydrogen bond, Pi-sulfur bond, as well as a hydrophobic (Pi-alkyl) bond. It also interacted with Ser125 via a conventional hydrogen bond (Table 4) & (Figure 28, left) and became closer to His447, Ser203, Phe297, Gly122, Phe338, and Asp74 (Figure 28, right). The close proximity to Ser203 and His447 from the catalytic triad, Phe295 from the acyl pocket, and Gly122 from the oxyanion hole might convert this pesticide to a more toxic and irreversible inhibitor via interaction with the enzyme CAS.

3.4.11. Docking of Phosphamidon into hAChE

The selected Phosphamidon-hAChE conformer (-5.0 Kcal/mol) stabilized via many types of interaction. Phosphamidon interacted with His381 via two carbon-hydrogen bonds (H-donor) as well as an unfavorable interaction with ligand phosphorous (Positive-Positive), Asp400 via an electrostatic (Attractive charge) bond, and with Arg525 via two conventional hydrogen bonds, (Table 4 & Figure 29, left) and become closer to Ala397, Ala528, Gln527, Arg393, Asp384, Tyr382 and Glu396 (Figure 29, right). Phosphamidon is the only OPs in this study that did not interact with the hAChE active site.

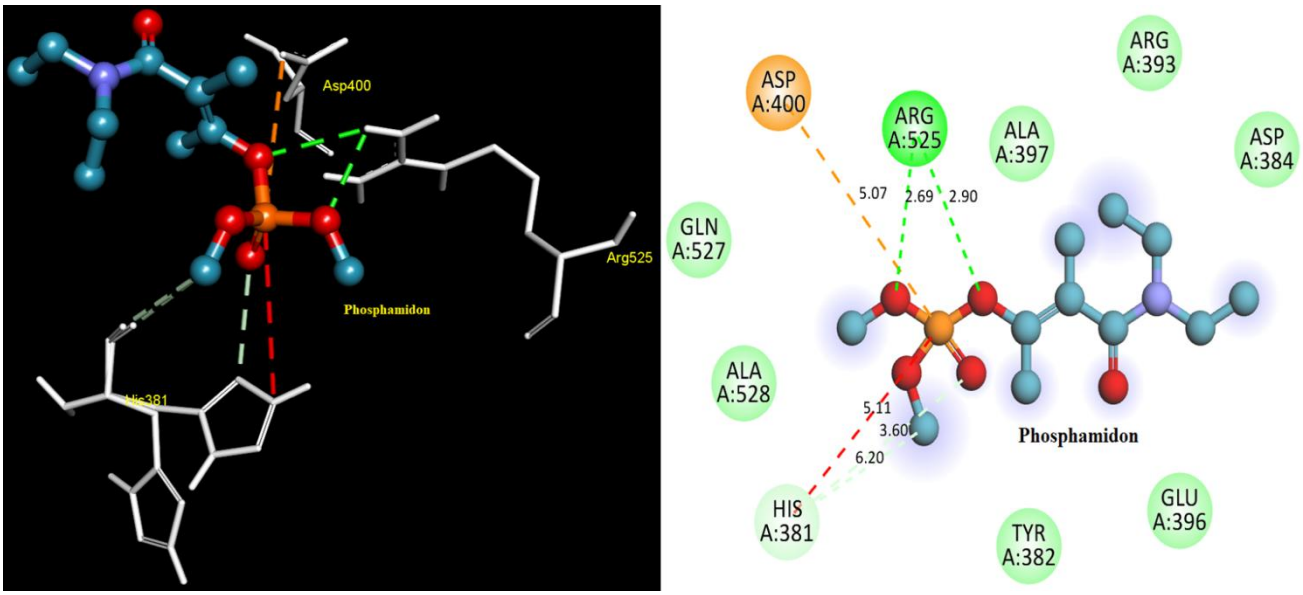

Figure 29: Interaction of Phosphamidon with hAChE active site: 3D structure of Phosphamidon-hAChE (left) and 2D structure (right) indicating types of interactions.

3.4.12. Docking of Phorate into hAChE

The selected Phorate-hAChE conformer (-4.8 Kcal/mol) stabilized via many types of interaction. Phorate interacted with Trp86 via a hydrophobic (Pi-sigma) and Phe297 via a Pi-sulfur bond. Phorate also interacted with PAS amino acid residues at Phe338 via a Pi-sulfur bond, Tyr337 via a Pi-sulfur bond, and Tyr124 via a conventional hydrogen bond. It also interacted with Asp74 via a hydrophobic (Pi-sigma) bond (Table 4 & Figure 30, left) and became closer to His447, Gly121, and Ser125 (Figure 30, right). The close proximity of His447 from the catalytic triad and Gly121 from the oxyanion hole might convert this pesticide to a more toxic and irreversible inhibitor via interaction with the enzyme CAS.

3.4.13. Docking of Terbufos into hAChE

The selected Terbufos-hAChE conformer (-4.5 Kcal/mol) stabilized via many types of interaction. Terbufos interacted with PAS amino acid residues at Tyr341 via a hydrophobic (Pi-Alkyl) bond and Trp286 via two electrostatic bonds (Pi-Cation), and a hydrophobic bond (Pi-Alkyl). Terbufos also interacted with Glu292 via an electrostatic bond (Pi-Cation) and Leu289 via a hydrophobic (Alkyl) bond (Table 4) & (Figure 31, left). It has also become closer to Phe338, Phe295, Phe297, Val294, Tyr72, Ser293, and Arg296 (Figure 31, right) which might make this pesticide a good hAChE reversible inhibitor.

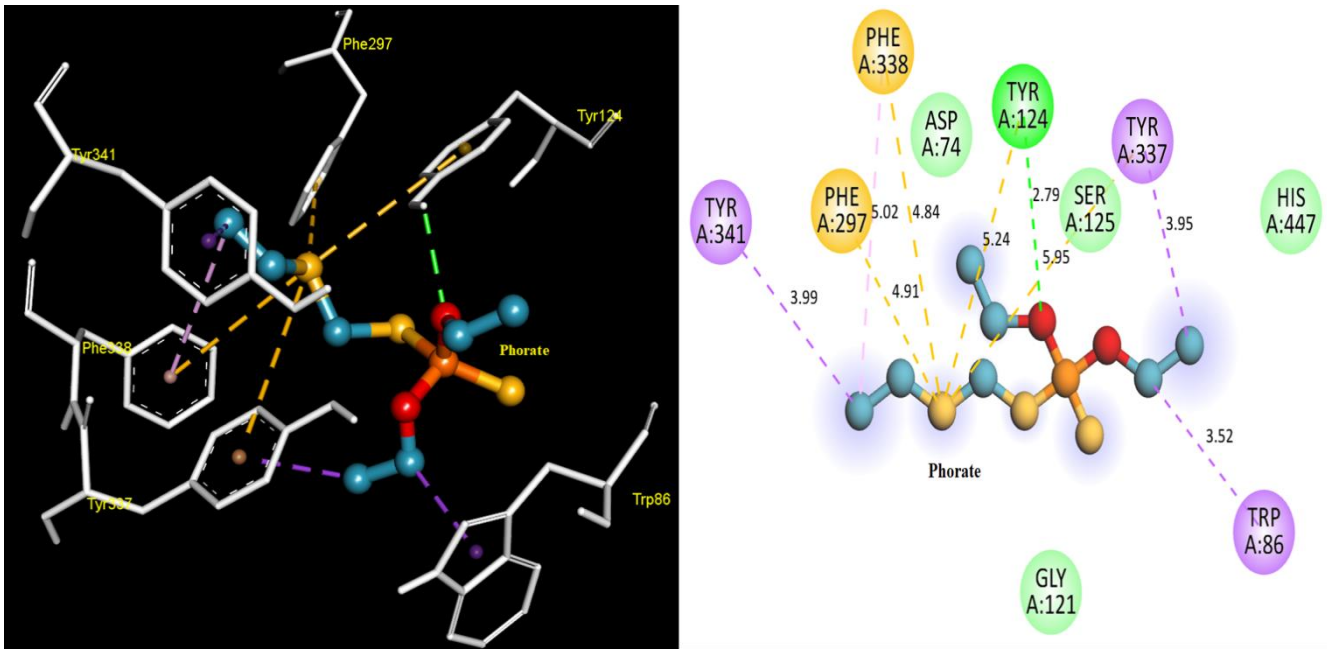

Figure 30: Interaction of Phorate with hAChE active site: 3D structure of Phorate-hAChE (left) and 2D structure (right) indicating types of interactions.

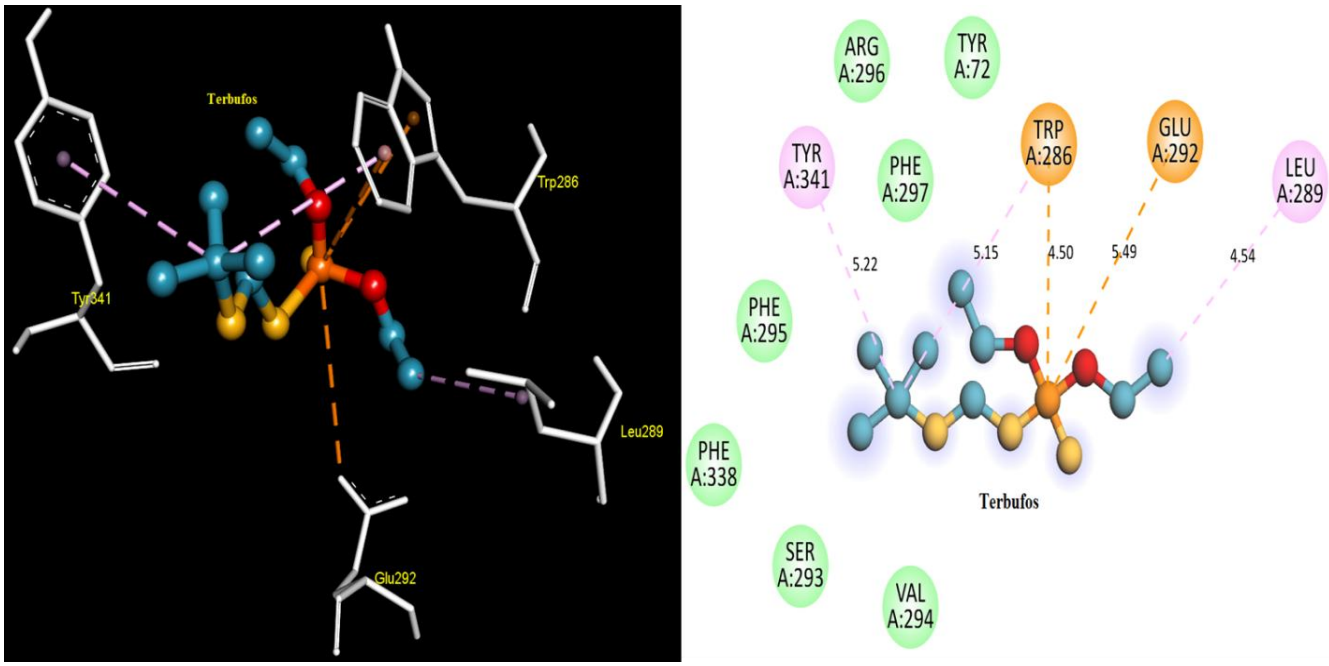

Figure 31: Interaction of Terbufos with hAChE active site: 3D structure of Terbufos-hAChE (left) and 2D structure (right) indicating types of interactions.

4. CONCLUSION

According to our results, the thirty common OPs are divided into three sets according to their behavioral binding with hAChE. The first set comprised eight OPs that could interact with both CAS and PAS of the hAChE active site and might be more toxic due to their irreversible inhibition. Additionally, the second set could be medium inhibitors as they did not interact with Ser203 at the catalytic triad of the hAChE active site. While the last set could be weak or irreversible inhibitors for hAChE, as they did not interact with CAS and mostly interacted with PAS amino acid. Further in vivo kinetics studies are importantly needed, especially on the last set to explore

new strategies for facing OPs toxicity and the treatment of neurodegenerative disorders, like Alzheimer's disease, as they might be hAChE irreversible inhibitors.

Acknowledgements
The authors are highly indebted to the support of the National Hepatology and Tropical Medicine Research Institute and the Central Agricultural Pesticides Laboratory-Agricultural Research Center.

Author Contributions:
Hala A. Abdelgaid: Resources, Methodology, Data curation, Formal analysis, Software, Investigation, Validation, Visualization, Writing–original draft. Khairy A. Ibrahim: Conceptualization, Project administration, Resources, Methodology, Data curation, Formal analysis, Software, Investigation, Validation, Visualization, Writing – Review & Editing.

Ethical Approval
Not applicable. This article does not contain any studies with human participants or animals performed by any of the authors.

Informed Consent
Not applicable.

Conflicts of interests
The authors declare that they have no conflicts of interest, competing financial interests or personal relationships that could have influenced the work reported in this paper.

Funding
This research did not receive any external funding like specific grant from funding agencies in the public, commercial, or nonprofit sectors.

Data and materials availability
The datasets used and/or analyzed during the current study are available from the corresponding author upon reasonable request.

REFERENCES

1. Cheung J, Rudolph MJ, Burshteyn F, Cassidy MS, Gary EN, Love J, Franklin MC, Height JJ. Structures of human acetylcholinesterase in complex with pharmacologically important ligands. Journal of medicinal chemistry. 2012;26; 55(22):10282-6. doi: 10.1021/JM300871X
2. Ekström F, Gottinger A, Forsgren N, Catto M, Iacovino LG, Pisani L, Binda C. Dual reversible coumarin inhibitors mutually bound to monoamine oxidase B and acetylcholinesterase crystal structures. ACS medicinal chemistry letters. 2022;18;13(3):499-506.
3. Ibrahim KA, Abdelgaid HA, Eleyan M, Khwanes SA, Abdel-Daim MM. Ethoprophos induces rats' brain injury and neurobehavioral impairment via transcriptional activation of glial fibrillary acidic protein and tubulin-associated unit even at the threshold inhibition of acetylcholinesterase: A 90-days study. Science of The Total Environment. 2021;10;777:146216. doi: 10.1016/j.scitotenv.2021.146216
4. Kiametis AS, Silva MA, Romeiro LA, Martins JB, Gargano R. Potential acetylcholinesterase inhibitors: molecular docking, molecular dynamics, and in silico prediction. Journal of molecular modeling. 2017; 23(2):67.doi: 10.1007/S00894-017-3228-9
5. Kumar S, Kaushik G, Dar MA, Nimesh S, Lopez-Chuken UJ, Villarreal-Chiu JF. Microbial degradation of organophosphate pesticides: a review. Pedosphere. 2018; 1;28(2):190-208. doi: 10.1016/S1002-0160(18)60017-7
6. Lindgren C, Forsgren N, Hoster N, Akfur C, Artursson E, Edvinsson L, Svensson R, Worek F, Ekström F, Linusson A. Broad-spectrum antidote discovery by untangling the reactivation mechanism of nerve-agent-inhibited acetylcholinesterase. Chemistry–A European Journal. 2022;15; 28(40):e202200678. doi: 10.1002/CHEM.202200678
7. Mangas I, Estevez J, Vilanova E, França TC. New insights on molecular interactions of organophosphorus pesticides with

esterases. Toxicology 2017;1;376:30-43. doi: 10.1016/J.TOX.2016.06.006

8. McGuire JR, Bester SM, Guelta MA, Cheung J, Langley C, Winemiller MD, Bae SY, Funk V, Myslinski JM, Pegan SD, Height JJ. Structural and biochemical insights into the inhibition of human acetylcholinesterase by G-series nerve agents and subsequent reactivation by HI-6. Chemical Research in Toxicology. 2021;4;34(3):804-16. doi: 10.1021/ACS.CHEMRESTOX.0C00406
9. Mdeni NL, Adeniji AO, Okoh AI, Okoh OO. Analytical evaluation of carbamate and organophosphate pesticides in human and environmental matrices: a review. Molecules. 2022;18;27(3):618. doi: 10.3390/MOLECULES27030618
10. O'Boyle NM, Banck M, James CA, Morley C, Vandermeersch T, Hutchison GR. Open Babel: An open chemical toolbox. Journal of cheminformatics. 2011;7;3(1):33. doi: 10.1186/1758-2946-3-33
11. Rosenfeld CA, Sultatos LG. Concentration-dependent kinetics of acetylcholinesterase inhibition by the organophosphate paraoxon. Toxicological sciences. 2006;1;90(2):460-9. doi: 10.1093/TOXSCI/KFJ094
12. Saxena AK, The Structural Hybrids of Acetylcholinesterase Inhibitors in the Treatment of Alzheimer's Disease: A Review. Alzheimer's & Neurodegenerative Diseases 2019;4:1–25. doi: 10.24966/AND-9608/100015
13. Shakil S, Khan R, Tabrez S, Alam Q, R. Jabir N, I. Sulaiman M, H. Greig N, A. Kamal M. Interaction of human brain acetylcholinesterase with cyclophosphamide: a molecular modeling and docking study. CNS & Neurological Disorders-Drug Targets-CNS & Neurological Disorders. 2011;1;10(7):845-8. doi: 10.2174/187152711798072365
14. Trott O, Olson AJ. AutoDock Vina: improving the speed and accuracy of docking with a new scoring function, efficient optimization, and multithreading. Journal of computational chemistry. 2010; 30;31(2):455-61. doi: 10.1002/JCC.21334